CESifo WORKING PAPERS

10404
2023

May 2023

Regional Productivity Network in the EU

Camilla Mastromarco, Laura Serlenga, Yongcheol Shin

CESifo

Impressum:

CESifo Working Papers
ISSN 2364-1428 (electronic version)
Publisher and distributor: Munich Society for the Promotion of Economic Research - CESifo GmbH
The international platform of Ludwigs-Maximilians University's Center for Economic Studies and the ifo Institute
Poschingerstr. 5, 81679 Munich, Germany
Telephone +49 (0)89 2180-2740, Telefax +49 (0)89 2180-17845, email office@cesifo.de
Editor: Clemens Fuest
https://www.cesifo.org/en/wp
An electronic version of the paper may be downloaded
· from the SSRN website: www.SSRN.com
· from the RePEc website: www.RePEc.org
· from the CESifo website: https://www.cesifo.org/en/wp

CESifo *Working Paper No. 10404*

Regional Productivity Network in the EU

Abstract

We develop a unified stochastic frontier model which controls for the local spatial correlation and the global factor dependence as well as parameter heterogeneity, simultaneously. We then propose the regional productivity network analysis to examine the diffusion impacts of the capital intensity on the labour productivity in the EU. We apply the proposed approach to the dataset consisting of 202 regions in the EU15 countries over 1980-2019, and convincingly unveil that the technological shock diffuses from efficient regions operating on or near the frontier to inefficient regions. This suggests that policies to enhance domestic absorption capacity appear better suited to net receivers of technological shocks whilst policies to attract more R&D investments are appropriate to their transmitters. In this regard we stress the importance of investing European funds in peripheral regions to address regional inequality and polarisation.

JEL-Codes: C130, C330, D240, O470.

Keywords: spatial stochastic frontier model with factors and heterogeneity, CCEX-IV estimator, regional productivity network analysis in the EU, efficiency clusters.

Camilla Mastromarco
University of Calabria / Italy
camilla.mastromarco@unical.it

Laura Serlenga
European Commission
lserlenga@gmail.com

Yongcheol Shin
University of York / United Kingdom
yongcheol.shin@york.ac.uk

May 1, 2023
We gratefully acknowledge many helpful interactions with Jia Chen, Matthew Greenwood-Nimmo, Rui Lin, Chaowen Zheng, and the comments of seminar participants at the University of York. Shin acknowledges partial financial support from the ESRC (Grant Reference: ES/T01573X/1). The usual disclaimer applies.

1 Introduction

An intense debate in the growth literature concerns with which countries/regions, that are increasingly economically integrated with the rest of the world, can maintain a sustainable economic growth (e.g. Jones (2016)). Consequently, there have been a vast number of studies focusing on how to incorporate the role of the global/local interdependence in explaining development and growth. Several studies have emphasised the importance of international technological spillovers as a major engine behind technological progress (e.g. Coe and Helpman, 1995; Eaton and Kortum, 2002; Barro and Sala-i-Martin, 2003; Howitt, 2000; Lucas, 1988, 1993). A few papers have also provided pervasive empirical evidence in favour of the spatial spillover effect and heterogeneity on the productivity and growth (e.g. Ramajo et al., 2008; Vogel, 2013) while the frontier analysis has recognised the importance of spillover effects stemming from either the spatial correlations or the global factor dependence (Mastromarco et al., 2016; Gude et al., 2018).

Output growth is typically explained as the accumulation of factor inputs and the growth of total factor productivity. This can be understood by viewing output growth from the perspective of a production possibility frontier where regions can be operating on or within the frontier, with the distance from the frontier representing inefficiency. A region's frontier can shift over time (technological change) or a region can move towards or away from the frontier (efficiency change). Moreover, a region can move along the frontier by changing inputs. So productivity growth can be made up of three components: technology, efficiency and input changes with the first two being the productivity change (e.g. Koop et al., 1999).

Most studies analysing the effect of spatial spillovers on productivity of countries/regions have employed the neoclassical production function model, e.g. Mankiw et al. (1992) (MRW). Ertur and Koch (2007) develop a spatially-augmented Solow model in cross-section that includes capital externalities (e.g. Arrow, 1962), and spatial externalities of knowledge/idea (e.g. Romer, 1990) so as to model technological interdependence. Shi and Lee (2016) show that the spatial Durbin terms also play an important role in explaining the growth convergence of 26 OECD countries. Fischer (2018) combines an MRW model with a spatial autoregressive specification for investigating the technological interdependence among European regions. Miranda et al. (2017) develop a growth model with interdependencies in the heterogeneous technological progress, capital and stock of knowledge that yields an empirical specification corresponding to the spatial Durbin dynamic panel data model with spatially weighted individual-specific effects, and propose the quasi-maximum likelihood (QML) estimation using a correlated random effects approach. See also Elhorst (2010), Liu et al. (2020) and Galli (2021).

Regarding the literature on the stochastic frontier models, several studies have also emphasised the importance of accommodating the spatial correlation in modelling technical efficiency. The seminal paper proposed by Druska and Horrace (2004), develops the panel data frontier model with autoregressive spatial errors and apply the Schmidt and Sickles (1984) estimator to calculate firm-specific efficiency scores without imposing any distributional assumption on inefficiency terms. Schmidt et al. (2009) show that the failure to control for the presence of cross-sectional correlation in the regional production data, may yield biased results in both direct and indirect impacts of each explanatory variable. Glass et al. (2016) developed a spatial autoregressive stochastic frontier model and propose a multi-stage pseudo MLE. Gude et al. (2018) extend this approach and develop a generalised spatial autoregressive stochastic frontier model with time-varying variables that influence the degree of the global spatial interaction. All these studies highlight that failure to account for the spatial dependence may result in biased estimates of efficiency scores.

The aforementioned studies do not explicitly accommodate the global cross-section dependence, usually charaterised by unobserved factors. Recently, some progresses have been made in modelling both local and global cross-section correlations through the joint analysis of spatial- and factor-based panel data models. Mastromarco et al. (2016) propose a technique for modelling stochastic frontier panels by combining the exogenous factor-based approach and an endogenous threshold selection mechanism. Bai and Li (2021) develops the QML estimation for a homogeneous spatial panel data model with common shocks. Using a similar model, Yang (2021) develops a consistent estimator that combines the common correlated effects (CCE) and instrumental variable (IV) estimation. See also Shi and Lee (2017), Lu (2022) and Kuersteiner and Prucha (2020) .

However, most studies still maintain the assumption that the slope parameters are homogeneous. In a data-rich environment, slope homogeneity is a restrictive assumption, as the strength and direction of spatial dependence between regions may vary over space. For instance, as a regional growth tends to be influenced by neighbours in a complex manner, such interlinkages render unrealistic the assumption of region's homogeneity (e.g. Vogel, 2013). In the analysis of cross-section growth regressions, the parameter homogeneity has been regarded restrictive (e.g. Durlauf, 2001; Canova, 2004; Ertur and Koch, 2007). In the spatial literature, Aquaro et al. (2021) and Shin and Thornton (2021) have explicitly allowed the slope parameters to be heterogeneous and develop the QML and the control function-based estimators. See also LeSage and Chih (2016) and Sun and Malikov (2018). Recently, Chen et al. (2022) develop the panel data model with the parameter heterogeneity that can accommodate both spatial dependence and common factors, and propose the CCEX-IV estimator that approximates factors by the cross-section averages of regressors and deals with the spatial endogeneity using the internally selected instrumental variables.

In this paper, as a main contribution, we develop a unified stochastic frontier model in which we control for parameter heterogeneity, local spatial dependence and global factor dependence, simultaneously. We then derive the corresponding empirical specification by the spatial Durbin stochastic frontier (SDSF) model with heterogeneous parameters and unobserved factors, in which technological interdependence is spatially dependent but technical inefficiencies are subject to the factor dependence.

We propose the comprehensive regional productivity diffusion network analysis in the EU as follows: First, we estimate the SDSF model consistently by the CCEX-IV estimator advanced by Chen et al. (2022). Next, we propose estimating individual (in)efficiencies using the approach by Cornwell et al. (1990), and construct the five efficiency clusters based on the regional efficiency rankings. Finally, we apply the GCM-based network analysis advanced by Greenwood-Nimmo et al. (2021) and Shin and Thornton (2021) and analyse the diffusion impacts of the capital intensity on the labour productivity across the five clusters.

We demonstrate the utility of our proposed approach with an application to the dataset consisting of 202 regions in the EU15 countries over the period, 1980–2019. From Cambridge Econometrics European Regional Database we collect annual observations on employment, hours worked, gross fixed capital formation and gross value added for NUTS3 EU15 regions. To capture technological proximity across the EU regions, we construct the spatial weighting matrix based on technological distance (e.g. Basile et al., 2012), reflecting the main idea that regions similar in technology proximity, will be more receptive to externally produced knowledge (e.g. Boschma, 2005).

The main empirical findings are summarised as follows: First, all individual coefficients are pronounced heterogeneous and significant, but mostly positive. Overall, there is strong evidence in favor of the positive technology spillover. Second, the higher values of heterogeneous spill-out effects, which capture the impacts of the capital intensity from region i on the labour productivity of all other regions, are concentrated in core regions. By contrast, the higher values of spill-in effects, which collect the impacts of the capital intensity from all other regions on the labour productivity of region i, are observed mostly in peripheral regions. Third, the regional efficiency ranking is broadly consistent with a core-periphery decomposition in the EU. The spatial pattern of efficiency is positively correlated with that of per capita GDP with the correlation at 0.85 in 2019, stronger than 0.74 in 1980. Fourth, polarisation and regional disparities tend to be more persistent recently, while productivity convergence occurs only in core regions with similar technologies. Furthermore, there is no evidence of regional efficiency convergence in the EU. This is in line with the European race for the best location. Finally, we show that the relative position in the dependence/influence space can provide a vivid measure of regional capabilities to spur and absorb productivity spillovers, unveiling that the technological shock diffuses from the efficient regions operating on or near the frontier to inefficient regions.

The proposed regional network analysis is shown to highlight the importance of explicitly modelling the production/efficiency network to better understand the main determinants behind the productivity growth, which will provide a valuable information for policymakers to promote sustainable long-term economic growth and reduce income disparities. Recent developments of endogenous growth theories emphasise the different roles that appropriate institutions and policies may play in either backward or advanced economies as well as the distinction between innovation activities and an adoption of existing technologies from the global production frontier (e.g. Acemoglu et al., 2006; Jones, 2016). In this regard we suggest that policies to enhance domestic absorption capacity appear better suited to technology adoption by net receivers of production technological shocks whilst policies to attract more investments in the high-skilled human capital and R&D are more appropriate to the transmitters of technological shocks. We also stress the importance of investing European funds in peripheral regions to address regional inequality and polarisation, because large differences in the production structure and the highly unequal distribution of technological capabilities in the EU regions would be self-reinforcing and intensifying polarisation and divergence without such coordinated policies.

The rest of the paper is organised as follows. Section 2 develops a unified stochastic frontier model that controls for parameter heterogeneity, local spatial and global factor dependence, simultaneously. Section 3 describes the CCEX-IV estimation methodology and proposes the regional productivity network analysis. Section 4 presents the main empirical results using the dataset for 202 regions in the EU15 countries. Section 5 concludes. The additional simulation and empirical results are relegated to the Online Appendix.

2 The Stochastic Frontier Model with Spatial and Factor Dependence

Following the research trends reviewed in Introduction, we develop the generalised stochastic frontier panel data model with spatial and factor dependence as well parameter heterogeneity. Consider the (heterogeneous) Cobb-Douglas production function in a region i:

$$Y_{it} = A_{it} K_{it}^{\alpha_{Ki}} H_{it}^{\alpha_{Hi}} L_{it}^{1-\alpha_{Ki}-\alpha_{Hi}} \quad \text{for } i = 1, ..., N, \ t = 1, ..., T, \tag{1}$$

where Y_{it} is the product of a region i at time t, L_{it} is the labor input, K_{it} is the gross fixed capital stock, H_{it} is the human capital, and A_{it} is the Hicks-neutral factor productivity. Letting the lower case letter be variables normalised by the size of the labor force (i.e. $y_{it} = Y_{it}/L_{it}$), then the production function can be written as

$$y_{it} = A_{it} k_{it}^{\alpha_{Ki}} h_{it}^{\alpha_{Hi}} \text{ for } i = 1, ..., N, \ t = 1, ..., T. \tag{2}$$

Mankiw et al. (1992) argue that technology created anywhere in the world of regions is immediately available in any region. They assume that $\ln A_{it} = a + \varepsilon_{it}$ where a is a constant term and ε is the iid idiosyncratic error, though they point out that this term reflects not just technology but region-specific influences on growth such as resource endowments, institutions and so on. In this regard, Fischer (2018) proposes the following functional form:

$$A_{it} = \Omega_t k_{it}^{\phi_K} h_{it}^{\phi_H} \prod_{j \neq i}^{N} A_{jt}^{\rho w_{ij}} \tag{3}$$

where Ω_t is technological knowledge, assumed to be identical in all regions and grows at a constant rate. The next two terms suppose that A_{it} of each region increases with per worker physical capital, k_{it}, reflecting the learning-by-doing process emphasised by Arrow (1962) and Romer (1986), and with per worker human capital, h_{it}, reflecting human capital externalities as underlined by Lucas (1988) . The last term serves to account for technological interdependence that A_{it} may depend on A_{jt} for $i, j = 1, ..., N$.

We aim to develop the heterogeneous spatially-augmented stochastic frontier model with unobserved factors by utilising the following extended model for A_{it}:

$$A_{it} = \Omega_{it} k_{it}^{\phi_{Ki}} h_{it}^{\phi_{Hi}} \prod_{j \neq i}^{N} A_{jt}^{\rho_i w_{ij}}. \tag{4}$$

The level of technology available in region i at time t, depends on unobserved individual/time specific stock of knowledge, (Ω_{it}), the level of technology embodied in physical and human capital per worker (k_{it} and h_{it}), and the spatial/network connectivity given by $\prod_{j \neq i}^{N} A_{jt}^{\rho_i w_{ij}}$. Next, we follow the frontier literature (e.g. Färe et al. (1994)), and decompose Ω_{it} into a technical inefficiency, u_{it}, and an idiosyncratic error, v_{it} that captures the stochastic nature of the frontier:

$$\Omega_{it} = \exp\left(-u_{it} + v_{it}\right) \tag{5}$$

Following Mastromarco et al. (2013) and Mastromarco et al. (2016), we propose the factor-based specification for modelling time-varying technical inefficiency as

$$u_{it} = \alpha_i + \boldsymbol{\lambda}_i' \boldsymbol{f}_t, \; i = 1, ..., N, \; t = 1, ..., T, \tag{6}$$

where α_i is (unobserved) individual effects of region i and $\boldsymbol{f}_t$ is an $r \times 1$ vector of unobserved factors, affecting all regions with heterogeneous loadings $\boldsymbol{\lambda}_i$. These time-varying factors are supposed to capture an exogenous technological change (e.g. Coelli and Battese, 1995; Ahn et al., 2007), and expected to provide a good proxy for nonlinear and complex trending patterns associated with the global/regional business-cycles.

Taking the log of (2) and combining it with (4)–(6), we show that the product of a region i is determined by the levels of per capita physical and human capital, but it also depends on spatial spillovers among regions as well as global factors. After some algebra, it is straightforward to derive the following heterogeneous stochastic frontier model with both spatial and factor dependence:

$$y_{it} = \rho_i \sum_{j=1}^{N} w_{ij} y_{jt} + \beta_{1i} k_{it} + \beta_{2i} h_{it} + \pi_{1i} \sum_{j=1}^{N} w_{ij} k_{jt} + \pi_{2i} \sum_{j=1}^{N} w_{ij} h_{jt} - u_{it} + v_{it} \tag{7}$$

This is the empirical specification of the theoretical model given by (2) and (4), and corresponds to the spatial Durbin panel data specification with unobserved factors and heterogeneous parameters, which we refer to as the SDSF model. This approach embodies a data generating process where the level of technology, A_{it} is spatially dependent and the technical inefficiency, u_{it} is subject to global factor dependence. First, spatial knowledge externalities involve technological interdependence among regions such that regions similar in the level of production technology have more capacity to reciprocate the production technology know-how. This similarity serves as channels for the diffusion of technology through $\prod_{j \neq i}^{N} A_{jt}^{\rho_i w_{ij}}$. Next, the capacity to assimilate common production knowledge, captured by efficiency, tends to depend on how each region is globally connected such that global factors drive regional efficiency through $(\alpha_i + \boldsymbol{\lambda}_i' \boldsymbol{f}_t)$. This is in line with the literature emphasising that the international catching-up process (changes in efficiency) are mainly achieved through the channels of global factors (e.g. Coe and Helpman, 1995; Eaton and Kortum, 2002; Caves, 2007; Iyer et al., 2008).

3 Estimation Methodology

For convenience, we rewrite the SDSF model, (7) as

$$y_{it} = \rho_i y_{it}^* + \boldsymbol{\beta}_i' \boldsymbol{x}_{it} + \boldsymbol{\pi}_i' \boldsymbol{x}_{it}^* + \varepsilon_{it}, \ i = 1, ..., N, \ t = 1, ..., T, \tag{8}$$

where y_{it} is the dependent variable of the ith spatial unit at time t, $\boldsymbol{x}_{it}$ is a $k \times 1$ vector of regressors with a $k \times 1$ vector of parameters, $\boldsymbol{\beta}_i$. Spatial interdependence across regions are captured via the spatial variables, $y_{it}^* \equiv \sum_{j=1}^{N} w_{ij} y_{jt} = \boldsymbol{w}_i' \boldsymbol{y}_t$ with $\boldsymbol{y}_t = (y_{1t}, ..., y_{Nt})'$ and $\boldsymbol{x}_{it}^* = (\boldsymbol{w}_i' \otimes \boldsymbol{I}_k) \boldsymbol{x}_t$ with $\boldsymbol{x}_t = (\boldsymbol{x}_{1t}', ..., \boldsymbol{x}_{Nt}')'$, and $\boldsymbol{w}_i = (w_{i1}, ..., w_{iN})'$ denotes an $N \times 1$ vector of (non-stochastic) spatial weights determined *a priori* with $w_{ii} = 0$. Notice that ε_{it} is the error components given by

$$\varepsilon_{it} = v_{it} - u_{it} = v_{it} - (\alpha_i + \boldsymbol{\lambda}_i' \boldsymbol{f}_t), \tag{9}$$

where v_{it} is the idiosyncratic error and u_{it} is the term measuring the (time-varying) technical inefficiency. α_i is (unobserved) region-specific effect and $\boldsymbol{f}_t$ is an $r \times 1$ vector of common factors affecting all regions with heterogeneous loadings $\boldsymbol{\lambda}_i$.

3.1 The CCEX-IV estimator

In order to consistently estimate the heterogeneous stochastic frontier panel data model with both spatial and factor dependence in (8), we propose the use of the CCEX-IV estimator advanced by Chen et al. (2022). Stacking (8) over t, we have:

$$\boldsymbol{y}_{i.} = \rho_i \boldsymbol{y}^*_{i.} + \boldsymbol{X}_{i.}\boldsymbol{\beta}_i + \boldsymbol{X}^*_{i.}\boldsymbol{\pi}_i + \boldsymbol{\varepsilon}_{i.} = \boldsymbol{Z}_{i.}\boldsymbol{\theta}_i + \boldsymbol{\varepsilon}_{i.}, \tag{10}$$

where $\boldsymbol{y}_{i.} = (y_{i1}, \ldots, y_{iT})'$, $\boldsymbol{y}^*_{i.} = (\boldsymbol{I}_T \otimes \boldsymbol{w}_i)\boldsymbol{y} = (y^*_{i1}, \ldots, y^*_{iT})'$ with $\boldsymbol{w}_i$ the i-th row of $\boldsymbol{W}$, $\boldsymbol{X}_{i.} = (\boldsymbol{x}_{i1}, \ldots, \boldsymbol{x}_{iT})'$, $\boldsymbol{X}^*_{i.} = (\boldsymbol{x}^*_{i1}, \ldots, \boldsymbol{x}^*_{iT})'$, $\boldsymbol{Z}_{i.} = (\boldsymbol{y}^*_{i.}, \boldsymbol{X}_{i.}, \boldsymbol{X}^*_{i.})$, $\boldsymbol{\theta}_i = (\rho_i, \boldsymbol{\beta}'_i, \boldsymbol{\pi}'_i)'$ and $\boldsymbol{\varepsilon}_{i.} = (\varepsilon_{i1}, \ldots, \varepsilon_{iT})'$. Using $\bar{\boldsymbol{x}}_t = N^{-1}\sum_{i=1}^N \boldsymbol{x}_{it}$ as factor proxies, we construct the following de-factorisation matrix:

$$\tilde{\boldsymbol{M}}_{\bar{\boldsymbol{X}}} = \boldsymbol{M}_{\bar{\boldsymbol{X}}} \otimes \boldsymbol{I}_N \quad \text{with} \quad \boldsymbol{M}_{\bar{\boldsymbol{X}}} = \boldsymbol{I}_T - \bar{\boldsymbol{X}}(\bar{\boldsymbol{X}}'\bar{\boldsymbol{X}})^+\bar{\boldsymbol{X}}', \tag{11}$$

where $\bar{\boldsymbol{X}} = (\bar{\boldsymbol{x}}_1, \ldots, \bar{\boldsymbol{x}}_T)'$ and $(\bar{\boldsymbol{X}}'\bar{\boldsymbol{X}})^+$ is the Moore-Penrose inverse of $\bar{\boldsymbol{X}}'\bar{\boldsymbol{X}}$. We construct the $NT \times \iota$ matrix of instrumental variables, denoted $\tilde{\boldsymbol{Q}} = (\boldsymbol{M}_{\bar{\boldsymbol{X}}} \otimes \boldsymbol{I}_N)\boldsymbol{Q}$, where the IVs can be obtained by $\boldsymbol{X}_{.t} = (\boldsymbol{x}_{1t}, \ldots, \boldsymbol{x}_{Nt})'$ and their higher order spatial lagged terms such that $\underset{NT\times\iota}{\boldsymbol{Q}} = (\boldsymbol{Q}'_{.1}, \ldots, \boldsymbol{Q}'_{.T})'$, where $\boldsymbol{Q}_{.t}$ is an $N \times \iota$ ($\iota \geq (k+1)$) matrix consisting of the ι columns of the IV set $(\boldsymbol{X}_{.t}, \ldots, \boldsymbol{W}^r\boldsymbol{X}_{.t}, \ldots)$ for each t and for $r = 0, 1, 2, \cdots$.

We can consistently estimate $\boldsymbol{\theta}_i$ by the individual CCEX-IV estimator given by

$$\hat{\boldsymbol{\theta}}_i = \left(\boldsymbol{Z}'_{i.}\boldsymbol{\Pi}_i\boldsymbol{Z}_{i.}\right)^{-1}\boldsymbol{Z}'_{i.}\boldsymbol{\Pi}_i\boldsymbol{y}_{i.}, \tag{12}$$

where $\boldsymbol{\Pi}_i = \tilde{\boldsymbol{Q}}_i(\tilde{\boldsymbol{Q}}'_i\tilde{\boldsymbol{Q}}_i)^{-1}\tilde{\boldsymbol{Q}}'_i$, $\tilde{\boldsymbol{Q}}_i = \boldsymbol{M}_{\bar{\boldsymbol{X}}}(\boldsymbol{I}_T \otimes \boldsymbol{b}'_i)\boldsymbol{Q}$, and $\boldsymbol{b}_i$ is the $N \times 1$ column vector with the i-th entry being 1 and 0 otherwise. Chen et al. (2022) show that as $(N, T) \to \infty$ and $T/N^2 \to 0$, then

$$\sqrt{T}(\hat{\boldsymbol{\theta}}_i - \boldsymbol{\theta}_i) \xrightarrow{d} N(\boldsymbol{0}, \boldsymbol{\Omega}_i), \; i = 1, ..., N$$

where a consistent estimator for $\boldsymbol{\Omega}_i$ is obtained by

$$\hat{\boldsymbol{\Omega}}_i = \left(\frac{\boldsymbol{Z}'_{i.}\boldsymbol{\Pi}_i\boldsymbol{Z}_{i.}}{T}\right)^{-1}\left(\frac{\boldsymbol{Z}'_{i.}\tilde{\boldsymbol{Q}}_i}{T}\right)\left(\frac{\tilde{\boldsymbol{Q}}'_i\tilde{\boldsymbol{Q}}_i}{T}\right)^{-1}\hat{\boldsymbol{\Sigma}}_i\left(\frac{\tilde{\boldsymbol{Q}}'_i\tilde{\boldsymbol{Q}}_i}{T}\right)^{-1}\left(\frac{\tilde{\boldsymbol{Q}}'_i\boldsymbol{Z}_{i.}}{T}\right)\left(\frac{\boldsymbol{Z}'_{i.}\boldsymbol{\Pi}_i\boldsymbol{Z}_{i.}}{T}\right)^{-1} \tag{13}$$

and $\hat{\boldsymbol{\Sigma}}_i$ is the robust estimator of $\boldsymbol{\Sigma}_i$ given by

$$\hat{\boldsymbol{\Sigma}}_i = \hat{\boldsymbol{\Sigma}}_{i,0} + \sum_{h=1}^{p_T}\left(1 - \frac{h}{p_T + 1}\right)\left(\hat{\boldsymbol{\Sigma}}_{i,h} + \hat{\boldsymbol{\Sigma}}'_{i,h}\right),$$

where $\hat{\boldsymbol{\Sigma}}_{i,h} = \sum_{t=h+1}^T \hat{e}_{it}\hat{e}_{i,t-h}\tilde{\boldsymbol{q}}_{it}\tilde{\boldsymbol{q}}'_{i,t-h}/T$, p_T is the bandwidth of the Bartlett kernel, $\hat{\boldsymbol{e}}_{i.} = \boldsymbol{M}_{\bar{\boldsymbol{X}}}(\boldsymbol{y}_{i.} - \boldsymbol{Z}_{i.}\hat{\boldsymbol{\theta}}_i) = (\hat{e}_{i1}, \ldots, \hat{e}_{iT})'$, and $\tilde{\boldsymbol{q}}_{it}$ is the $\iota \times 1$ vector of the t-th column of $\tilde{\boldsymbol{Q}}'_i$.

Next, we consider the CCEX-IV mean group (MG) estimator for $\boldsymbol{\theta} = E(\boldsymbol{\theta}_i)$ given by[1]

$$\hat{\boldsymbol{\theta}}_{MG} = \frac{1}{N}\sum_{i=1}^{N}\hat{\boldsymbol{\theta}}_i. \tag{14}$$

Then, it follows that as $(N, T)\to\infty$,

$$\sqrt{N}\left(\hat{\boldsymbol{\theta}}_{MG} - \boldsymbol{\theta}\right) \xrightarrow{d} N\left(\mathbf{0}, \boldsymbol{\Omega}_{MG}\right),$$

where $\boldsymbol{\Omega}_{MG}$ can be consistently estimated by the nonparametric estimator (Pesaran, 2006):

$$\hat{\boldsymbol{\Omega}}_{MG} = \hat{\boldsymbol{\Omega}}_{\xi} = \frac{1}{N-1}\sum_{i=1}^{N}(\hat{\boldsymbol{\theta}}_i - \hat{\boldsymbol{\theta}}_{MG})(\hat{\boldsymbol{\theta}}_i - \hat{\boldsymbol{\theta}}_{MG})'. \tag{15}$$

Remark 1. *Econometric methods have been developed for dealing with the spatial and factor dependence, separately. The spatial endogeneity can be resolved by using QML (Lee, 2004) or IV/GMM estimation (Kelejian and Prucha, 1998, 1999). The common factors can be approximated by the PC estimates (Bai, 2009) or the cross-section averages of the variables (Pesaran, 2006). A few studies have recently combined both approaches, e.g. Bai and Li (2014, 2021), Mastromarco et al. (2016), Shi and Lee (2017), Kuersteiner and Prucha (2020) and Yang (2021). Here, we follow the CCEX-IV approach by Chen et al. (2022), who suggest the use of $\bar{\boldsymbol{x}}_t$ only as proxies for unobserved factors. Though they do not consider the spatial Durbin panel data model explicitly, it is straightforward to extend their approach under the maintained assumption of exogeneity of the regressors, $\boldsymbol{x}_{it}$. To develop consistent estimation of the $(2k+1)\times 1$ parameters, $\boldsymbol{\theta}_i = (\rho_i, \boldsymbol{\beta}_i', \boldsymbol{\pi}_i')'$ in (10), we should address two sources of endogeneity: the correlation between $\boldsymbol{x}_{it}$ and factors and the correlation of the spatial lagged term, y_{it}^* with both factors and idiosyncratic error, v_{it}. Notice that the CCEX approach requires the weaker condition, $T/N^2 \to 0$ whilst the CCE approach, using both $\bar{y}_t$ and $\bar{\boldsymbol{x}}_t$, requires the stronger condition, $T/N \to 0$.*

3.2 The estimation of technical efficiency

The production frontier is defined as the maximum attainable output given the level of inputs in such that an inefficiency becomes zero by construction. To evaluate the time-varying inefficiency we follow the approach by Schmidt and Sickles (1984) and Cornwell et al. (1990).[2]

[1]Notice that the pooled estimator is inconsistent in the presence of spatial parameter heterogeneity, as shown by Chen et al. (2022).

[2]Cornwell et al. (1990) propose the following time-varying specification: $y_{it} = \boldsymbol{\beta}'\boldsymbol{x}_{it} + \alpha_{it} + \varepsilon_{it}$ with $\alpha_{it} = \boldsymbol{\delta}_i'\boldsymbol{w}_t$, where $\boldsymbol{w}_t = \left(1, t, t^2\right)'$ and $\boldsymbol{\delta}_i = (\delta_{i1}, \delta_{i2}, \delta_{i3})'$. They estimate $\boldsymbol{\delta}_i$ by regressing the residual, $(y_{it} - \hat{\boldsymbol{\beta}}'\boldsymbol{x}_{it})$

We proxy unobserved factors by $\bar{\boldsymbol{x}}_t$ and derive the augmented model of (8) by

$$y_{it} = \rho_i y_{it}^* + \boldsymbol{\beta}_i' \boldsymbol{x}_{it} + \boldsymbol{\pi}_i' \boldsymbol{x}_{it}^* + \boldsymbol{\psi}_i' \bar{\boldsymbol{x}}_t + \alpha_i^* + v_{it}^*,\ i = 1, ..., N,\ t = 1, ..., T \tag{16}$$

Provided that the augmented model (16) is asymptotically equivalent to the model (8), then technical inefficiency can be obtained by

$$e_{it} = \max_j (\alpha_j^* + \boldsymbol{\psi}_j' \bar{\boldsymbol{x}}_t) - (\alpha_i^* + \boldsymbol{\psi}_i' \bar{\boldsymbol{x}}_t),\ i, j = 1, ..., N,\ t = 1, ..., T \tag{17}$$

To consistently estimate e_{it}, we need to derive consistent estimates of heterogeneous parameters, α_i^* and $\boldsymbol{\psi}_i$ for $i = 1, ..., N$. Replacing $\boldsymbol{\theta}_i = (\rho_i, \boldsymbol{\beta}_i', \boldsymbol{\pi}_i')'$ by $\hat{\boldsymbol{\theta}}_i$ in (16), we obtain:

$$\tilde{y}_{it} = \alpha_i^* + \boldsymbol{\psi}_i' \bar{\boldsymbol{x}}_t + \tilde{v}_{it},\ i = 1, ..., N,\ t = 1, ..., T \tag{18}$$

where $\tilde{y}_{it} = y_{it} - \hat{\rho}_i y_{it}^* - \hat{\boldsymbol{\beta}}_i' \boldsymbol{x}_{it} - \hat{\boldsymbol{\pi}}_i' \boldsymbol{x}_{it}^*$, and $\tilde{v}_{it} = v_{it}^* - (\hat{\boldsymbol{\theta}}_i - \boldsymbol{\theta}_i)' \boldsymbol{z}_{it} = v_{it} + o_p(1)$. For sufficiently large T, we can estimate α_i^* and $\boldsymbol{\psi}_i$ consistently by the OLS estimator, denoted $\hat{\alpha}_i^*$ and $\hat{\boldsymbol{\psi}}_i$, from the regression of (18) for each i. Hence, the individual time-varying technical inefficiency can be consistently estimated by

$$\hat{e}_{it} = \max_j (\hat{\alpha}_j^* + \hat{\boldsymbol{\psi}}_j' \bar{\boldsymbol{x}}_t) - (\hat{\alpha}_i^* + \hat{\boldsymbol{\psi}}_i' \bar{\boldsymbol{x}}_t),\ i, j = 1, ..., N,\ t = 1, ..., T \tag{19}$$

Finally, the time-varying individual and common technical efficiencies, denoted τ_{it}, can be estimated by

$$\hat{\tau}_{it} = \exp(-\hat{e}_{it}) \tag{20}$$

Remark 2. *This is the approach adopted by Mastromarco et al. (2016). Here time-varying (in)efficiencies are measured by evaluating individual effects and factors components. By placing the unit with the largest value on the frontier, the individual inefficiency is estimated as the exponential of the difference between the effect of the best performing unit and that of each of the other units in the sample. Importantly, this approach can avoid the restrictive distributional assumption on efficiency and the over-parameterisation (Cornwell et al., 1990). Another advantage lies in that the spatio-temporal behaviour of inefficiency is so flexible that it increases or decreases and its cross-sectional membership changes over time.*

3.3 Productivity network analysis

Stacking the individual SDSF regressions, (8) over N, we have the following spatial system representation:

$$\begin{aligned} \boldsymbol{y}_t &= \boldsymbol{P}\boldsymbol{W}\boldsymbol{y}_t + \boldsymbol{B}\boldsymbol{x}_t + \boldsymbol{\Pi}(\boldsymbol{W} \otimes \boldsymbol{I}_k)\boldsymbol{x}_t + \boldsymbol{\varepsilon}_t \\ \boldsymbol{\varepsilon}_t &= \boldsymbol{v}_t - \boldsymbol{u}_t \text{ with } \boldsymbol{u}_t = \boldsymbol{\alpha} + \boldsymbol{\Lambda}\boldsymbol{f}_t \end{aligned} \tag{21}$$

on $\boldsymbol{w}_t$ for each i. The fitted values provide an estimate of α_{it}, denoted $\hat{\alpha}_{it}$. Then, they propose estimating the time-varying individual technical inefficiency by $\max_j \hat{\alpha}_{jt} - \hat{\alpha}_{it}$ for $i, j = 1, ..., N$ and $t = 1, ..., T$.

where $\boldsymbol{y}_t = (y_{1t}, ..., y_{Nt})'$, $\boldsymbol{x}_t = (\boldsymbol{x}'_{1t}, ..., \boldsymbol{x}'_{Nt})'$, $\boldsymbol{f}_t = (f_{1t}, ..., f_{rt})'$, $\boldsymbol{\Lambda} = (\boldsymbol{\lambda}_1, ..., \boldsymbol{\lambda}_N)'$, $\boldsymbol{W}$ is the $N \times N$ spatial weights matrix, and $\boldsymbol{P} = diag(\rho_1, ..., \rho_N)$, $\boldsymbol{B} = diag(\boldsymbol{\beta}'_1, ..., \boldsymbol{\beta}'_N)$, $\boldsymbol{\Pi} = diag(\boldsymbol{\pi}'_1, ..., \boldsymbol{\pi}'_N)$ are diagonal matrices consisting of the heterogeneous parameters.

Notice that the coefficients on the regressors in (8) cannot be interpreted as the marginal effects. For homogeneous static panels, LeSage and Pace (2009) propose an average of the diagonal elements of the matrix of partial derivatives as a summary measure of direct effect whilst the cumulative sum of off-diagonal elements is interpreted as indirect effects. In heterogeneous panels, LeSage and Chih (2016) enrich the interpretation of the elements of the partial derivative matrix, noticing that the off-diagonal elements in the rows are different from those in the columns.

To define a measure of the direct and indirect effects of the regressors on the dependent variable, we consider the following transformation of (21):

$$\begin{aligned} \boldsymbol{y}_t &= (\boldsymbol{I}_N - \boldsymbol{PW})^{-1} (\boldsymbol{B} + \boldsymbol{\Pi}(\boldsymbol{W} \otimes \boldsymbol{I}_k))\boldsymbol{x}_t + (\boldsymbol{I}_N - \boldsymbol{PW})^{-1} \boldsymbol{\varepsilon}_t \qquad (22) \\ &= (\boldsymbol{I}_N - \boldsymbol{PW})^{-1} (\boldsymbol{B} + \boldsymbol{\Pi}(\boldsymbol{W} \otimes \boldsymbol{I}_k))\boldsymbol{x}_t + (\boldsymbol{I}_N - \boldsymbol{PW})^{-1} \boldsymbol{v}_t - (\boldsymbol{I}_N - \boldsymbol{PW})^{-1} (\boldsymbol{\alpha} + \boldsymbol{\Lambda}\boldsymbol{f}_t) \end{aligned}$$

where the term $(\boldsymbol{I} - \boldsymbol{PW})^{-1}$ links the dependent variable to the regressors $\boldsymbol{x}_t$ and inefficiency terms. We construct heterogeneous direct, spill-in and spill-out effects for the ith region as

- Heterogeneous Direct Effect (HDE): the direct effect of the inputs on the output, given by the ith diagonal element of $(\boldsymbol{I}_N - \boldsymbol{PW})^{-1} (\boldsymbol{B} + \boldsymbol{\Pi}(\boldsymbol{W} \otimes \boldsymbol{I}_k))$.

- Heterogeneous Spill-in Effect (HSI): the sum of the effects of the inputs from all the other regions on the ouput in the ith region, given by ith row-sum minus ith diagonal element of $(\boldsymbol{I}_N - \boldsymbol{PW})^{-1} (\boldsymbol{B} + \boldsymbol{\Pi}(\boldsymbol{W} \otimes \boldsymbol{I}_k))$.

- Heterogeneous Spill-out Effect (HSO): the sum of the effects of the effect from the ith region on the output in all the other regions, given by the ith column-sum minus ith diagonal element of $(\boldsymbol{I}_N - \boldsymbol{PW})^{-1} (\boldsymbol{B} + \boldsymbol{\Pi}(\boldsymbol{W} \otimes \boldsymbol{I}_k))$.

Remark 3. *For the network-oriented approach in this section, we need only $\sqrt{T}$-consistent estimators of the individual heterogeneous parameters. A pooled or mean group estimator will net out heterogeneous signs and, therefore, fails to examine the relative importance of individual nodes beyond what is assumed ex ante via $\boldsymbol{W}$. For the mean group estimator, although consistency and asymptotic normality could be established under the random parameter assumption, in many practical applications, there is no economic reason to expect the coefficients of the model to share a common sign (e.g. Shin and Thornton, 2021).*

Our approach may operate at two extremes: (i) complete aggregation, where the $N(N-1)$ bilateral linkages among N individual regions are aggregated into the single indices (e.g.

Diebold and Yılmaz, 2014), and (ii) no aggregation, where the $N(N-1)$ bilateral linkages are studied at the individual regional level. We follow the GCM approach proposed by Greenwood-Nimmo et al. (2021) and introduce intermediate levels of aggregation by analysing the $R(R-1)$ bilateral linkages among R groups. We express the $N \times N$ matrix, $(\boldsymbol{I}_N - \boldsymbol{PW})^{-1}(\boldsymbol{B} + \boldsymbol{\Pi}(\boldsymbol{W} \otimes \boldsymbol{I}_k))$ as

$$\underset{(N\times N)}{\mathbf{C}} = \begin{bmatrix} \phi_{1\leftarrow 1} & \cdots & \phi_{1\leftarrow N_1} & \phi_{1\leftarrow N_1+1} & \cdots & \phi_{1\leftarrow N_1+N_2} & \cdots & \phi_{1\leftarrow N} \\ \vdots & \ddots & \vdots & \vdots & \ddots & \vdots & \ddots & \vdots \\ \phi_{N_1\leftarrow 1} & \cdots & \phi_{N_1\leftarrow N_1} & \phi_{N_1\leftarrow N_1+1} & \cdots & \phi_{N_1\leftarrow N_1+N_2} & \cdots & \phi_{N_1\leftarrow N} \\ \phi_{N_1+1\leftarrow 1} & \cdots & \phi_{N_1+1\leftarrow N_1} & \phi_{N_1+1\leftarrow N_1+1} & \cdots & \phi_{N_1+1\leftarrow N_1+N_2} & \cdots & \phi_{N_1+1\leftarrow N} \\ \vdots & \ddots & \vdots & \vdots & \ddots & \vdots & \ddots & \vdots \\ \phi_{N_1+N_2\leftarrow 1} & \cdots & \phi_{N_1+N_2\leftarrow N_1} & \phi_{N_1+N_2\leftarrow N_1+1} & \cdots & \phi_{N_1+N_2\leftarrow N_1+N_2} & \cdots & \phi_{N_1+N_2\leftarrow N} \\ \vdots & \ddots & \vdots & \vdots & \ddots & \vdots & \ddots & \vdots \\ \phi_{N\leftarrow 1} & \cdots & \phi_{N\leftarrow N_1} & \phi_{N\leftarrow N_1+1} & \cdots & \phi_{N\leftarrow N_1+N_2} & \cdots & \phi_{N\leftarrow N} \end{bmatrix}. \tag{23}$$

The (k, ℓ)th block in (23), denoted as $\mathbf{B}_{k\leftarrow\ell}$ for $k, \ell = 1, ..., R$, is given by:

$$\underset{(N_k\times N_\ell)}{\mathbf{B}_{k\leftarrow\ell}} = \begin{bmatrix} \phi_{\tilde{N}_k+1\leftarrow\tilde{N}_\ell+1} & \cdots & \phi_{\tilde{N}_k+1\leftarrow\tilde{N}_\ell+N_\ell} \\ \vdots & \ddots & \vdots \\ \phi_{\tilde{N}_k+N_k\leftarrow\tilde{N}_\ell+1} & \cdots & \phi_{\tilde{N}_k+N_k\leftarrow\tilde{N}_\ell+N_\ell} \end{bmatrix}, \tag{24}$$

where $\widetilde{N}_k = \sum_{j=1}^{k-1} N_j$ for $k = 2, \ldots, R$, and $\widetilde{N}_1 = 0$. We evaluate the sum of the elements of $\mathbf{B}_{k\leftarrow\ell}$ and normalise it by the average number of regions in the pair as:

$$\psi_{k\leftarrow\ell} = \frac{1}{0.5(N_k + N_\ell)} \boldsymbol{\iota}'_{N_k} \mathbf{B}_{k\leftarrow\ell} \boldsymbol{\iota}_{N_\ell}, \tag{25}$$

where $\boldsymbol{\iota}_{N_k}$ is an $N_k \times 1$ column vector of ones. Then, we can construct the following $R \times R$ connectedness matrix at the group level:

$$\underset{(R\times R)}{\mathbf{C}_R} = \begin{bmatrix} \psi_{1\leftarrow 1} & \psi_{1\leftarrow 2} & \cdots & \psi_{1\leftarrow R} \\ \psi_{2\leftarrow 1} & \psi_{2\leftarrow 2} & \cdots & \psi_{2\leftarrow R} \\ \vdots & \vdots & \ddots & \vdots \\ \psi_{R\leftarrow 1} & \psi_{R\leftarrow 2} & \cdots & \psi_{R\leftarrow R} \end{bmatrix}. \tag{26}$$

It is straightforward to derive the direct, spill-in and spill-out effects at the group level using (26), denoted GDE, GSI and GSO, by

$$GDE_i = \psi_{i\leftarrow i};\ GSI_i = \sum_{j=1, j\neq i}^{R} \psi_{i\leftarrow j};\ GSO_i = \sum_{j=1, j\neq i}^{R} \psi_{j\leftarrow i}.$$

We construct the group net effect (GNE) by the difference between GSO and GSI, which enables us to distinguish between net-transmitting and net-receiving groups, respectively.

Finally, we follow Shin and Thornton (2021) and construct the External Motivation (EM) and Systemic Influence (SI) indices given by

$$EM_i = \frac{GSI_i}{ATOT_{i\leftarrow\bullet}}; \quad SI_i = \frac{GNE_i}{TNP_i}, \tag{27}$$

where $ATOT_{i\leftarrow\bullet} = \sum_{j=1}^{R} |\psi_{i\leftarrow j}|$ is the absolute row-sum for group i, and $TNP_i = 0.5\sum_{i=1}^{N} |NE_i|$ is the total absolute net effects. EM_i measures the relative importance and direction of GSI in determining the conditions in the ith regional efficiency cluster while SI_i captures the systemic influence of the ith group.[3]

Remark 4. *In the empirical application, we apply the regional productivity network analysis to the five efficiency clusters constructed using the regional efficiencies ranking. We demonstrate that the coordinate pair (EM_i, SI_i) will provide a vivid representation of efficiency cluster's relative position in the EU productivity network. The identification of this regional productivity network is important for understanding the main channel of productivity growth. The presence of interconnections between regions plays an important role, functioning as potential propagation mechanism of productivity shocks. We document evidence that there is the tendency for efficiency clusters to gather along a line from northwest to southeast. An efficiency cluster in the northwest (southeast) quadrant would be one for which spill-outs (spill-ins) outweigh spill-ins (spill-outs), leading to a positive (negative) net connectedness which corresponds to the technologically superior (inferior) efficiency cluster.*

4 Empirical Results

Our data are sourced from "EUROSTAT, Cambridge Econometrics European Regional Database (ERD)," covering EU27 countries (not including Croatia). While the original EU15 data covers the period 1980-2019, the data for the 12 new member states are only available during 1990-2019. To employ the longer period (1980-2019), we consider the dataset consisting of 202 regions in the EU15 (Austria (AT), Belgium (BE), Germany (DE), Denmark (DK), Greece (EL), Spain (ES), Finland (FI), France (FR), Ireland (IE), Italy (IT), Luxembourg (LU), the Netherlands (NL), Portugal (PT), Sweden (SE), United Kingdom (UK)).

[3] EM_i and SI_i stay within $[-1, 1]$. If $EM_i \to 1(-1)$, then the output in group i is dominated by positive (negative) GSIs, as opposed to direct effects. If group i receives contradictory spill-ins and/or if GSI is small in comparison to direct effects, then $EM_i \to 0$. If $0 \leq SI_i \leq 1$ ($-1 \leq SI_i \leq 0$), then group i is a net shock transmitter (receiver). If SI_i is close to zero, then group i is neutral with its GSOs matching GSIs.

Regional output is constructed as regional gross value added (GVA) plus taxes less subsidies on products, measured at constant euro price in 2005. Labour is measured as total employment in thousands, and capital (in millions Euros) is constructed using the perpetual inventory method (PIM).[4] All three variables are logged before we estimate the following spatial Durbin production function with unobserved factors:

$$\begin{aligned} y_{it} &= \rho_i y_{it}^* + \beta_i k_{it} + \pi_i k_{it}^* + \varepsilon_{it}, \\ \varepsilon_{it} &= v_{it} - u_{it} = v_{it} - (\alpha_i + \boldsymbol{\lambda}_i' \boldsymbol{f}_t), \; i = 1, \dots, N; \; t = 1, \dots, T, \end{aligned} \tag{28}$$

where y_{it} is the logged labor productivity (output/labor) and k_{it} the logged capital intensity (capital/labor) for region i at time t. The spatial lagged term and the Durbin term are given by $y_{it}^* = \sum_{j=1}^N w_{ij} y_{it}$ and $k_{it}^* = \sum_{j=1}^N w_{ij} k_{it}$ with w_{ij} being the (i, j)-th element of the spatial weighting matrix. To capture technological proximity among EU regions we construct the spatial weighting matrix based on technological distance (e.g. Basile et al., 2012). We construct the dissimilarity measure by

$$tech_{ij} = \frac{\sum_{k=1}^{K} |s_{ik} - s_{jk}|}{\sum_{k=1}^{K} (s_{ik} + s_{jk})}, \; i, j = 1, ..., N \tag{29}$$

where s_{ik} is the employment share of sector k at region i with $K = 6$.[5] In the literature on the economic structure this measure of dissimilarity has been preferred to the Euclidean distance (e.g. De Benedictis and Tajoli, 2007). We then construct the row-sum normailised weights matrix with inverse technological distance, denoted W_{tech} as a measure of technological proximity. The main idea is that regions similar in technology proximity will be more receptive to externally produced knowledge. Several studies suggest that being technologically similar to other regions increases the likelihood to absorb new knowledge produced outside, because

[4] PIM is necessitated by the lack of the capital stock data in all EU regions. For an individual region, the capital stock is constructed as $K_t = K_{t-1} (1 - \theta) + I_t$, where I_t is investment (gross fixed capital formation measured at constant euro price in 2005) and θ is the rate of depreciation assumed to be 6% (e.g. Hall and Jones, 1999; Iyer et al., 2008). Repair and maintenance are assumed to keep the physical production capabilities of an asset constant during its lifetime. Initial capital stocks are constructed, assuming that capital and output grow at the same rate. Specifically, for region with investment data beginning in 1980, we set the initial stock, $K_{1980} = I_{1980}/ (g + \theta)$, where g is the 10-year output growth rate from 1980 to 1990. Estimated capital stock includes both residential and non-residential capital.

[5] In the Cambridge Econometrics database, the NACE2 Sectors are aggregated as follows: 1. Agriculture, Forestry and Fishing; 2. Industry - excluding Construction; 3. Construction; 4. Wholesale, Retail, Transport, Accommodation and Food Services, Information and Communication; 5. Financial and Business Services; 6. Non-market Services.

the higher is the likelihood that the production knowledge can be understood and efficiently adopted (e.g. Bode, 2004; Aldieri and Cincera, 2009).

To conduct the regional productivity network analysis, we proceed as follows.

- First, we estimate the spatial Durbin stochastic frontier (SDSF) model, (28) with heterogeneous parameters and unobserved factors by the CCEX individual and MG estimators, using $\hat{\boldsymbol{F}}_t = (1, \bar{k}_t)'$ as proxies for the individual effect and unobserved factors. We then employ $(\tilde{\boldsymbol{X}}, \tilde{\boldsymbol{X}}^*, \tilde{\boldsymbol{X}}^{2*})$ as the IVs for the spatial lagged term, y^*_{it} where $\tilde{\boldsymbol{X}} = (\boldsymbol{M}_{\hat{\boldsymbol{F}}} \otimes \boldsymbol{I}_N)\boldsymbol{X}$, $\tilde{\boldsymbol{X}}^* = (\boldsymbol{M}_{\hat{\boldsymbol{F}}} \otimes \boldsymbol{I}_N)(\boldsymbol{I}_T \otimes \boldsymbol{W})\boldsymbol{X}$ and $\tilde{\boldsymbol{X}}^{2*} = (\boldsymbol{M}_{\hat{\boldsymbol{F}}} \otimes \boldsymbol{I}_N)(\boldsymbol{I}_T \otimes \boldsymbol{W}^2)\boldsymbol{X}$ with $\boldsymbol{M}_{\hat{\boldsymbol{F}}} = \boldsymbol{I}_T - \hat{\boldsymbol{F}}(\hat{\boldsymbol{F}}'\hat{\boldsymbol{F}})^{-1}\hat{\boldsymbol{F}}'$ and $\boldsymbol{X} = (\boldsymbol{X}'_{.1}, \ldots, \boldsymbol{X}'_{.T})'$ (see (12) and (14)).

- Next, as the stochastic frontier model implicitly assumes the presence of the common global frontier (all units inside the production set may reach the maximum product given a common technology), we propose estimating individual (in)efficiencies using the MG estimator (see the derivations in (16)–(20)).[6] Based on the regional efficiency ranking, we construct the five efficiency clusters where the first quintile is the group with the highest efficiencies and the 5th is the group with the lowest efficiencies.

- Finally, we apply the generalised connectedness measure (GCM) and the output network analysis advanced by Greenwood-Nimmo et al. (2021) and Shin and Thornton (2021) to the five efficiency clusters, so as to analyse the diffusion impacts of the capital intensity on the labour productivity in the EU regions (see Section 3.3).

In Table 1 we present the MG estimation results for the SDSF model in (28). For comparison we report the estimation results for the spatial Durbin panel data model with fixed effects only using the spatial FE-IV estimator.[7] Notice that when computing the MG estimates, we exclude 11 regions with their spatial coefficient outside (-1,1). As an ex-post diagnostic, we report the CD test (Pesaran, 2015) results applied to the residuals and the CSD exponent estimate, denoted α (Bailey et al., 2016). For the spatial FE-IV estimator, the CD test convincingly rejects the null of weak CSD while α is estimated at 0.972, suggesting the presence of strong CSD. On the contrary, the null of weak CSD is not rejected with a much lower estimate of α at 0.5 for the CCEX-IV estimator. Hence, the spatial FE-IV estimation results are likely to be biased and unreliable (e.g. Pesaran, 2006; Bai, 2009). In what follows, we focus on the CCEX-IV estimation results, from which we find that all coefficients are positive and statistically significant. There is strong evidence in favor of the positive spillover ($\hat{\rho}_{MG} = 0.319$). The own regional impact ($\hat{\beta}_{MG} = 0.44$) of the capital

[6] In particular, we obtain: $\tilde{y}_{it} = y_{it} - \hat{\rho}_{MG} y^*_{it} - \hat{\boldsymbol{\beta}}'_{MG}\boldsymbol{x}_{it} - \hat{\boldsymbol{\pi}}'_{MG}\boldsymbol{x}^*_{it}$ in (18).

[7] We first apply the within transformation to get rid of individual effects, and apply the IV estimation using the same set of instruments as in the the CCEX-IV estimator.

intensity on the labour productivity is also substantial and larger than the neighbour impacts ($\hat{\pi}_{MG} = 0.315$).

Table 1 about here

We investigate some stylised patterns of the cross-sectional distributions of the heterogeneous coefficients on y^*_{it}, k_{it}, and k^*_{it}, respectively. Figure 1 displays the kernel densities of the individual coefficients, $\hat{\rho}_i$, $\hat{\beta}_i$ and $\hat{\pi}_i$ while Table 2 presents the descriptive statistics. Out of a total of 202 regions, we observe that $\hat{\rho}_i > 1$ only for 11 regions while they become negative but mostly insignificant (24 out of 30). This implies that most EU regions tend to gain a positive spillover due to technological proximity. Further, we observe that negative and low ρ coefficients are observed mostly in peripheral regions of Ireland, Greece, Norway, Spain, Portugal and Sweden, while the higher spatial coefficients are clustered in central and northern core regions (see Figure 2). This suggests that the positive spatial productivity networks occur across the regions if they share technological proximity. This evidence provides the support for the central role played by core regions in spreading technological innovation and the relatively low productivity of EU peripheries, the latter of which may reflect the fact that relatively poor infrastructure in peripheral regions would create barriers to the technology diffusion.

Table 2 and Figures 1 and 2 about here

Next, we analyse the spatial patterns of the impacts of the (own) capital intensity on the labour productivity (β). They are quite heterogeneous but mostly positive (around 15% are negative, see Figure 1). Negative β coefficients are mostly observed in peripheral regions in Greece, Portugal and Spain (Figure 3), where their poor infrastructure hampers a country's ability to trade in the global economy and adopt the technology diffusion. Interestingly, we find that the impacts of the capital intensity tend to be smaller in some core regions in Germany, the Netherlands, Norway and Sweden than in peripheral regions in Italy and Spain (Figure 3). This may imply that the labour productivity is likely to be largely enhanced by high-tech investments in rich and core regions, that is in line with the evidence that these regions are more likey to adopt R&D intensive production technology. Furthermore, the higher β coefficient combined with the lower ρ coefficient observed for some peripheral regions may suggest that the production technology in these regions is more likely to be dominated by (inferior) domestic production inputs rather than efficient production technology transferred from core regions.

Figure 3 about here

Finally, we analyse the spatial patterns of the impacts of (neighbours) capital intensity on the labour productivity (π). Overall, they are positive but more heterogeneous and volatile than domestic counterparts (β) (see Figure 1). These effects tend to be more positive in the higher income regions of Belgium, Germany, Italy, the Netherlands, Norway and Spain, which are able to adopt advanced production technology (Figure 4).

Figure 4 about here

Notice, however, that the coefficients in the model (28) are no longer interpreted as the marginal impacts. In this regard, we follow LeSage and Chih (2016) and Shin and Thornton (2021), and analyse the cross-sectional distributions of the heterogeneous direct effect (HDE), heterogeneous spill-in effect (HSI), and heterogeneous spill-out effect (HSO) of the capital intensity on the labour productivity, respectively. We display kernel densities of HDE, HSI and HSO in Figure 5, and present their spatial distributions in Figures 6 and 7. The higher direct effects are concentrated in the UK and Spanish regions while the lower HDEs are largely observed in regions in Greece, Portugal, Italy, Sweden and Norway. HSIs show quite a different pattern as the higher effects are displayed in Germany, Italy, Spain, Portugal and Sweden while the UK and Greece produce the lower values. Finally, the spatial pattern of HSO is somewhat similar to that of HDE and core regions in UK, Finland, Germany, France, Spain and Italy display high values. It is important to highlight that the higher values of HSO, which capture the sum of the impacts of the capital intensity from region i on the labour productivity of all other regions, are mostly concentrated in central and northern core regions, whilst the higher values of HSI, which collects the sum of the impacts of the capital intensity from all other regions on the labour productivity of region i, are largely observed in peripheral regions in Italy, Spain and Portugal. This contrasting evidence demonstrates the central role played by core regions in spreading technological innovations to the less productive peripheral regions. Under EU policy agenda, the low income regions have always drawn considerable attention due to their economic and social problems. Recently, however, middle-income trapped regions have also attracted interests (Diemer et al., 2022), because they have experienced lengthy periods of low growth, weak productivity and employment loss. Our evidence may help the policy makers to identify the core regions, which may boost, through technological diffusion, productivity growth to economically trapped regions.

Table 3 and Figures 5–7 about here

We turn to the estimation of technical efficiency as described in Section 3.2. Under the maintained assumption that there is a common EU production frontier, we estimate the SDSF model, (28) by the CEEX-IV MG estimator, and evaluate individual efficiencies as in (19) and (20). According to the average efficiency level of each region over the full sample period reported in Table 4, we group the regions by the five efficiency clusters in descending order ($R = 5$). In Figure 8 we display the distribution of the five efficiency clusters across countries. Apart from Luxembourg with the only region, Denmark and Ireland contain the higher proportion of regions belonging to the top quintile. On the other hand, the higher proportions of regions belonging to the bottom quintile, are concentrated in Mediterranean countries, i.e. Portugal, Spain and Greece. Remarkably, this efficiency ranking is broadly consistent with the core-periphery regional decomposition in the EU.

Table 4 and Figure 8 about here

Table 5 presents the MG estimation results of the SDSF model for these 5 efficiency clusters. The impacts of the capital intensity on the labour productivity (β) tend to be in descending order, the strongest (0.55) in the 1st quintile cluster and the weakest (0.17) in the 5th cluster. On the other hand, the reverse pattern is observed for the Durbin coefficients (π). Finally, the spatial coefficients (ρ) exhibit slightly inverse-U shape with the 1st quintile exhibiting the weakest impact (0.2). Combining the patterns of ρ and π, we may conclude that the relatively inefficient clusters are more likely to be influenced by technology spillover from efficiency clusters. This is especially so for peripheral regions of Mediterranean countries, which mostly populate the lowest quintile.

Table 5 about here

Tables 6 and 7 present the regional efficiency rankings at the first (1980) and the last period (2019), respectively. We also display the spatial distributions of efficiency levels in Figure 9. In 1980 the top quintile of efficiency distribution contains mostly core regions from Belgium, Denmark, Germany, Greece, Ireland, Italy, the Netherlands, Sweden and the UK, whereas in 2019, the top quintile consists of core regions from Belgium, France, Germany, Ireland, the Netherlands, Sweden and the UK (the seven regions).[8] On the other hand, the bottom quintile consists of the border regions from Greece, Italy, Finland, Portugal, Spain, Sweden and the UK in 1980, whilst it manly consists of the regions from Greece, Portugal, Spain and Southern Italy in 2019. This provides a support that inefficient regions have recently become more concentrated in Mediterranean countries. During the whole period, the regions of the major cities did not register any significant change in terms of efficiency ranking, with the exception of the Lisbon region. On the contrary, technical efficiencies showed improvements only for some peripheral areas in Austria, Germany, the UK and the Nordic countries, whilst those in the Mediterranean countries worsened, confirming the growing regional inequality.

[8]Indeed, during this period, the British regions were able to become more productive and diffuse production technological spillovers.

Tables 6–7 and Figure 9 about here

Figure 10 displays the spatial distributions of regional per capita GDP in the first and last periods,[9] revealing that the level of regional disparities remains high as documented in EU and OECD (2019),OECD (2022). Over the full sample period, the Northern and the UK regions registered the highest growth rates of the labour productivity whereas the Mediterranean regions (especially, Greece) became stagnant even with negative growth rates, see European Commission and Inclusion (2019) and OECD (2021). Globalisation and technological progress have produced important macroeconomic benefits in knowledge-intensive sectors. This has mainly advantaged large cities where the high-value added services became more concentrated OECD (2019). However, this concentration/agglomeration raises equity concerns, making a regional convergence more challenging (Moretti, 2021). A growing literature documents the emergence of subnational economic clubs of development, consisting of regions with wide differences in dynamics of income, employment, industrial composition, education, productivity, innovation, urbanization and demography. This is generating a Europe of different speeds. Labour mobility also fails to reduce territorial inequality. Within-country migration trends in Europe have remained relatively low over the last three decades (Iammarino et al., 2017; European Commission and Inclusion, 2019). The COVID pandemic could also aggravate regional inequalities. For instance, despite a worse sanitary situation in the North, Southern Italian regions recorded the same employment loss during the first pandemic wave (Arbolino and Caro, 2021). The main reason is that poor regions have relatively fewer workers who can telework (IMF, 2020). Fundamentally, due to less-diversified economies and weaker institutions, these regions may struggle to reallocate the resources, leaving them more exposed to economic shocks.

Figure 10 about here

In Figure 11 we present the evolution of the GDP per capita across the five efficiency clusters. Within each cluster, we evaluate the quintile share ratio (QR) as the ratio of the top 20% to the bottom 20% quintile of the per capita GDP distribution, that represents a measure of the polarisation of income distribution.[10] Remarkably, the most inefficient regions in the 5th quintile are the most polarised. Regional disparities in the EU significantly declined until the global financial crisis, but renewed divergence has been observed in its aftermath, see OECD (2021). Even the regions in the first and the second efficient clusters exhibited an increasing polarisation over the last decade. Hence, we may conclude that this wide-spread

[9] Notice that the spatial pattern of efficiency is significantly and positively correlated with that of per capita GDP; 0.74 in 1980 and 0.85 in 2019.

[10] It captures the phenomenon of clustering around extreme poles. The more the distribution is polarised, the higher is the quintile share ratio.

polarisation, which started even before the financial crisis but intensified over the last decade, mainly reflects the global/European 'race for the best location'.

Figure 11 about here

To further investigate whether there is any evidence of regional efficiency convergence in the EU, we evaluate the probability of moving from one cluster to the other clusters over time. Figure 12 displays the transition probability matrix.[11] Perfect immobility will follow if the transition matrix becomes an identity matrix whilst perfect mobility might determine any matrix with zeros on the diagonal (no one ends where they started) or everyone has an equal probability of winding up in the various possible slots next period, regardless of starting positions. We find very little evidence of mobility across the five clusters, suggesting that there is evidence of a sluggish technological catch-up among the EU regions.

Figure 12 about here

Our findings suggest that polarisation and regional disparities tend to persist among the EU regions, while productivity convergence occurs only among core regions with similar technologies. This is in line with the previous studies, highlighting the importance of detecting the main drivers behind regional productivity growth to spur catching-up process of poorer EU regions (e.g. Quah, 1997; Magrini, 1999; Fiaschi et al., 2018). Moreover, several regions with efficiency level close or below the EU average, seem to be stuck in a "middle-low income trap".[12] The manufacturing sector in these regions is much smaller and weaker while their innovation system is not strong enough (e.g. Iammarino et al., 2017). To improve their performance, multiple changes need to occur at the same time: a stronger export-orientation, a shift into new sectors and activities, a boost to research and innovation, an increase in education and training, and an improvement in the business environment. Our evidence conveys the important policy recommendation: the richer regions may diffuse good management practices and production technological shocks to the poorer ones.

Finally, we conduct the network analysis as described in Section 3.3. We are particularly interested in investigating the productivity connectedness across the EU regions. To this end we apply the CGM network analysis of the causal impacts of the capital intensity

[11] The transition probability from one state to another is evaluated as $p_{ij} = \Pr(X_t = i | X_{t-1} = j) = \frac{N_{ij}}{\sum_{j=1}^{n} N_{ij}}$, where N_{ij} is the cell count and $\sum_{j=1}^{n} N_{ij}$ is the row sum.

[12] As noticed by Diemer et al. (2022), traps are part of the family of concepts that consider the possibilities for lower-income economies to catch-up with the leaders by virtue of the gradual narrowing of their income and productivity gaps (e.g. Fagerberg, 1994; Fagerberg and Godinho, 2004). Trap models are especially concerned with a particular breakdown of the catch-up process, consisting of growth slowdowns after a period of rapid take-off growth.

on the labour productivity to the five efficiency clusters in the EU. This analysis enables us to examine the role of each efficiency cluster in the diffusion of technological shocks. Table 8 reports the direct, spill-in, spill-out effects of the capital intensity on the labour productivity across the five efficiency clusters. The direct effects are substantially large for all clusters (higher than 60%) except for the 5th cluster (35%). Spill-out effects dominate spill-in effects for efficient clusters while the opposite pattern is observed for inefficient clusters. Consequently, the net effect is positive for the 1st and 2nd clusters, close to 0 for the 3rd cluster, but negative for the 4th and 5th clusters. This implies that the more efficient clusters (mostly corresponding to core regions) are the influential transmitter of production input shocks whereas the less efficient clusters become net receivers. Interestingly, we observe that the middle efficiency clusters 3 and 4 are more active in terms of bivariate interactions (the highest SI is observed for cluster 4 while the highest SO for cluster 3).

Table 8 about here

Next, we analyse how dependent is the ith efficiency cluster on external conditions from other clusters and to what extent the ith cluster influences or is influenced by the system as a whole. EM_i measures the relative importance and direction of spill-in effects in determining the conditions in the ith cluster while SI_i captures the systemic influence of the ith cluster, see (27). Figure 13 displays the coordinate pair (EM_i, SI_i) that will provide a vivid representation of the relative position of the five efficiency cluster in the EU regional productivity network. We find that the external motivation is always positive across all clusters. Remarkably, the five efficiency clusters tend to lay along a line from north-west to south-east, since positive spill-ins contribute negatively to a cluster's net effect. For the regions in the top efficient clusters spill-outs dominate spill-ins, which leads to a positive net connectedness. Thus, these clusters are the influential net transmitters of production input shocks. Conversely, the regions in the bottom inefficient clusters become the passive receivers of production shocks since their spill-ins outperform spill-outs, leading to a negative net connectedness. Our regional productivity network analysis can unveil that the technological shock diffuses from the better performing regions operating on or near the production frontier to inefficient regions operating well below the production frontier. This demonstrates that the relative position in the dependence-influence space can make an intuitive measure of capability to spur and absorb productivity spillovers.

Figure 13 about here

Our main empirical findings have the important policy implications. Recent developments of endogenous growth theories emphasise the different roles that appropriate institutions and policies may play in either backward or advanced economies as well as the distinction between innovation activities and an adoption of existing technologies from the global production frontier (e.g. Acemoglu et al., 2006; Jones, 2016). In this regard we suggest that policies to enhance domestic absorption capacity appear better suited to technology adoption by net receivers of technological shocks whilst policies to attract more investments in the high-skilled human capital and R&D are more appropriate to the transmitters of production technological shocks (e.g. Vandenbussche et al., 2006).

5 Conclusions

We have developed a unified stochastic frontier model which controls for the local spatial correlation and the global factor dependence as well as parameter heterogeneity, simultaneously, and derived the corresponding empirical specification by the spatial Durbin stochastic frontier (SDSF) model with heterogeneous parameters and unobserved factors, in which technological interdependence is spatially dependent while technical inefficiencies are subject to the global factor dependence.

We proposed the regional productivity diffusion network analysis in the EU as follows: First, we estimate the SDSF model consistently by the CCEX-IV estimator recently advanced by Chen et al. (2022). Next, we propose estimating individual (in)efficiencies using the approach by Cornwell et al. (1990), and construct the five efficiency clusters based on the regional efficiency rankings. Finally, we conduct the GCM-based network analysis, and analyse the diffusion impacts of the capital intensity on the labour productivity in the EU regions. We demonstrate the utility of our proposed approach with an application to the dataset consisting of 202 regions in the EU15 countries over the period, 1980–2019.

The proposed regional network analysis in the EU highlights the importance of explicitly modelling the production/efficiency network to better understand the main determinants behind the sustainable productivity growth. We suggest that policymakers should promote regional productivity growth by establishing the necessary network infrastructure and by providing incentives to support the development of domestic innovative capabilities conducive to absorb new technology advances. We also stress the importance of investing European funds in peripheral regions to address regional inequality and polarisation. Without such coordinated policies, large differences in the production structure and the highly unequal distribution of technological capabilities in the EU regions would be self-reinforcing and intensifying polarisation and divergence. In this regard, the European funding “Next Generation EU” should aim to build a more resilient, sustainable and digital friendly Europe.

References

Acemoglu, D., Aghion, P., and Zilibotti, F. (2006). Distance to Frontier, Selection, and Economic Growth. *Journal of the European Economic Association*, 4(1):37–74.

Ahn, S. C., Lee, Y. H., and Schmidt, P. (2007). Stochastic frontier models with multiple time-varying individual effects. *Journal of Productivity Analysis*, 27(1):1–12.

Aldieri, L. and Cincera, M. (2009). Geographic and technological R&D spillovers within the triad: micro evidence from US patents. *The Journal of Technology Transfer*, 34(2):196–211.

Aquaro, M., Bailey, N., and Pesaran, M. H. (2021). Estimation and inference for spatial models with heterogeneous coefficients: An application to us house prices. *Journal of Applied Econometrics*, 36(1):18–44.

Arbolino, R. and Caro, P. D. (2021). Can the eu funds promote regional resilience at time of covid-19? insights from the great recession. *Journal of Policy Modeling*, 43(1):109–126.

Arrow, K. J. (1962). The economic implications of learning by doing. *The Review of Economic Studies*, 29(3):155–173.

Bai, J. (2009). Panel data models with interactive fixed effects. *Econometrica*, 77(4):1229–1279.

Bai, J. and Li, K. (2014). Spatial panel data models with common shocks. mimeo., University of Columbia.

Bai, J. and Li, K. (2021). Dynamic spatial panel data models with common shocks. *Journal of Econometrics*, 224(1):134–160. Annals Issue: PI Day.

Bailey, N., Kapetanios, G., and Pesaran, M. H. (2016). Exponent of Cross-Sectional Dependence: Estimation and Inference. *Journal of Applied Econometrics*, 31(6):929–960.

Barro, R. J. and Sala-i-Martin, X. (2003). *Economic Growth, 2nd Edition*, volume 1 of *MIT Press Books*. The MIT Press.

Basile, R., Capello, R., and Caragliu, A. (2012). Technological interdependence and regional growth in europe: proximity and synergy in knowledge spillovers. *Papers in Regional Science*, 91:697–722.

Bode, E. (2004). The spatial pattern of localized r&d spillovers: An empirical investigation for germany. *Journal of Economic Geography*, 4:43–64.

Boschma, R. (2005). Proximity and innovation: A critical assessment. *Regional Studies*, 39(1):61–74.

Canova, F. (2004). Testing for convergence clubs in income per capita: A predictive density approach. *International Economic Review*, 45(1):49–77.

Caves, R. E. (2007). *Multinational Enterprise and Economic Analysis*. Cambridge Surveys of Economic Literature. Cambridge University Press, 3 edition.

Chen, J., Shin, Y., and Zheng, C. (2022). Estimation and inference in heterogeneous spatial panels with a multifactor error structure. *Journal of Econometrics*, 229(1):55–79.

Coe, D. and Helpman, E. (1995). International r&d spillovers. *European Economic Review*, 39(5):859–887.

Coelli, T. and Battese, G. (1995). A model for technical inefficiency effects in a stochastic frontier production function for panel data. *Empirical Economics*, 20:325–32.

Cornwell, C., Schmidt, P., and Sickles, R. C. (1990). Production frontiers with cross-sectional and time-series variation in efficiency levels. *Journal of Econometrics*, 46(1):185–200.

De Benedictis, L. and Tajoli, L. (2007). Economic integration and similarity in trade structures. *Empirica*, 34:117–137.

Diebold, F. X. and Yılmaz, K. (2014). On the network topology of variance decompositions: Measuring the connectedness of financial firms. *Journal of Econometrics*, 182(1):119–134.

Diemer, A., Iammarino, S., Rodríguez-Pose, A., and Storper, M. (2022). The regional development trap in europe. *Economic Geography*, 98(5):487–509.

Druska, V. and Horrace, W. C. (2004). Generalized moments estimation for spatial panel data: Indonesian rice farming. *American Journal of Agricultural Economics*, 86(1):185–198.

Durlauf, S. (2001). Manifesto for a growth econometrics. *Journal of Econometrics*, 100(1):65–69.

Eaton, J. and Kortum, S. (2002). Technology, geography, and trade. *Econometrica*, 70(5):1741–1779.

Elhorst, J. P. (2010). Applied spatial econometrics: Raising the bar. *Spatial Economic Analysis*, 5(1):9–28.

Ertur, C. and Koch, W. (2007). Growth, technological interdependence and spatial externalities: Theory and evidence. *Journal of Applied Econometrics*, 22(6):1033–1062.

European Commission, Directorate-General for Employment, S. A. and Inclusion (2019). *Employment and social developments in Europe 2019 : sustainable growth for all : choices for the future of Social Europe*. Publications Office.

Fagerberg, J. (1994). Technology and international differences in growth rates. *Journal of Economic Literature*, 32(3):1147–1175.

Fagerberg, J. and Godinho, M. (2004). *Innovation and Catching-Up*, pages 514–544. Oxford University Press.

Fiaschi, D., Gianmoena, L., and Parenti, A. (2018). Spatial club dynamics in european regions. *Regional Science and Urban Economics*, 72:115–130. New Advances in Spatial Econometrics: Interactions Matter.

Fischer, M. M. (2018). Spatial externalities and growth in a mankiw-romer-weil world: Theory and evidence. *International Regional Science Review*, 41(1):45–61.

Färe, R., Grosskopf, S., Norris, M., and Zhang, Z. (1994). Productivity growth, technical progress, and efficiency change in industrialized countries. *The American Economic Review*, 84(1):66–83.

Galli, F. (2021). A spatial durbin stochastic frontier model introducing spillover effects in the determinants of firms' efficiency. Working Paper 3924100, SRNN.

Glass, A. J., Kenjegalieva, K., and Sickles, R. C. (2016). A spatial autoregressive stochastic frontier model for panel data with asymmetric efficiency spillovers. *Journal of Econometrics*, 190(2):289–300.

Greenwood-Nimmo, M., Nguyen, V. H., and Shin, Y. (2021). Measuring the connectedness of the global economy. *International Journal of Forecasting*, 37(2):899–919.

Gude, A., Álvarez, I., and Orea, L. (2018). Heterogeneous spillovers among Spanish provinces: a generalized spatial stochastic frontier model. *Journal of Productivity Analysis*, 50(3):155–173.

Hall, R. E. and Jones, C. I. (1999). Why do some countries produce so much more output per worker than others? Working Paper 6564, NBER.

Howitt, P. (2000). Endogenous growth and cross-country income differences. *American Economic Review*, 90(4):829–846.

Iammarino, S., Rodríguez-Pose, A., and Storper, M. (2017). Why regional development matters for europe's economic future, regional and urban policy. Working Paper 07/2017, EU.

IMF (2020). Front matter. *IMF Staff Country Reports*, 2020(324).

Iyer, K. G., Rambaldi, A. N., and Tang, K. K. (2008). Efficiency externalities of trade and alternative forms of foreign investment in oecd countries. *Journal of Applied Econometrics*, 23(6):749–766.

Jones, C. (2016). Chapter 1 - the facts of economic growth. In Taylor, J. B. and Uhlig, H., editors, *Handbook of Macroeconomics*, volume 2, pages 3–69. Elsevier.

Kelejian, H. H. and Prucha, I. R. (1998). A generalized spatial two-stage least squares procedure for estimating a spatial autoregressive model with autoregressive disturbances. *Journal of Real Estate Finance and Economics*, 17:99–121.

Kelejian, H. H. and Prucha, I. R. (1999). A generalized moments estimator for the autoregressive parameter in a spatial model. *International Economic Review*, 40:509–533.

Koop, G., Osiewalski, J., and Steel, M. F. J. (1999). The components of output growth: A stochastic frontier analysis. *Oxford Bulletin of Economics and Statistics*, 61(4):455–487.

Kuersteiner, G. M. and Prucha, I. R. (2020). Dynamic spatial panel models: Networks, common shocks, and sequential exogeneity. *Econometrica*, 88(5):2109–2146.

Lee, L.-F. (2004). Asymptotic distributions of quasi-maximum likelihood estimators for spatial autoregressive models. *Econometrica*, 72:1899–1925.

LeSage, J. and Pace, R. K. (2009). *Introduction to spatial econometrics*. Chapman and Hall/CRC.

LeSage, J. P. and Chih, Y.-Y. (2016). Interpreting heterogeneous coefficient spatial autoregressive panel models. *Economics Letters*, 142:1–5.

Liu, X., Sun, T., and Feng, Q. (2020). Dynamic spatial spillover effect of urbanization on environmental pollution in china considering the inertia characteristics of environmental pollution. *Sustainable Cities and Society*, 53:101903.

Lu, L. (2022). Simultaneous spatial panel data models with common shocks. *Journal of Business & Economic Statistics*, 0(0):1–16.

Lucas, R. E. (1988). On the mechanics of economic development. *Journal of Monetary Economics*, 22(1):3–42.

Lucas, R. E. (1993). Making a miracle. *Econometrica*, 61(2):251–272.

Magrini, S. (1999). The evolution of income disparities among the regions of the european union. *Regional Science and Urban Economics*, 29(2):257–281.

Mankiw, N. G., Romer, D., and Weil, D. N. (1992). A Contribution to the Empirics of Economic Growth. *The Quarterly Journal of Economics*, 107(2):407–437.

Mastromarco, C., Serlenga, L., and Shin, Y. (2013). Globalisation and technological convergence in the EU. *Journal of Productivity Analysis*, 40(1):15–29.

Mastromarco, C., Serlenga, L., and Shin, Y. (2016). Modelling technical efficiency in cross sectionally dependent stochastic frontier panels. *Journal of Applied Econometrics*, 31(1):281–297.

Miranda, K., Martínez-Ibañez, O., and Manjón-Antolín, M. (2017). Estimating individual effects and their spatial spillovers in linear panel data models: Public capital spillovers after all ? *Spatial Statistics*, 22:1–17.

Moretti, E. (2021). The effect of high-tech clusters on the productivity of top inventors. *American Economic Review*, 111(10):3328–75.

OECD (2019). *OECD Regional Outlook 2019: Leveraging Megatrends for Cities and Rural Areas*. OECD.

OECD (2021). *OECD Regional Outlook 2021: No Ordinary Recovery Navigating the Transition*. OECD.

OECD (2022). *OECD Regions and Cities at a Glance 2022*. OECD.

Pesaran, M. H. (2006). Estimation and inference in large heterogeneous panels with a multifactor error structure. *Econometrica*, 74(4):967–1012.

Pesaran, M. H. (2015). Testing weak cross-sectional dependence in large panels. *Econometric Reviews*, 34(6):1089–1117.

Quah, D. T. (1997). Empirics for growth and distribution: Stratification, polarization, and convergence clubs. *Journal of Economic Growth*, 2(1):27–59.

Ramajo, J., Márquez, M. A., Hewings, G. J., and Salinas, M. M. (2008). Spatial heterogeneity and interregional spillovers in the european union: Do cohesion policies encourage convergence across regions? *European Economic Review*, 52(3):551–567.

Romer, P. M. (1986). Increasing returns and long-run growth. *Journal of Political Economy*, 94(5):1002–1037.

Romer, P. M. (1990). Endogenous technological change. *Journal of Political Economy*, 98(5):S71–S102.

Schmidt, A. M., Moreira, A. R. B., Helfand, S. M., and Fonseca, T. C. O. (2009). Spatial stochastic frontier models: accounting for unobserved local determinants of inefficiency. *Journal of Productivity Analysis*, 31(2):101–112.

Schmidt, P. and Sickles, R. C. (1984). Production frontiers and panel data. *Journal of Business & Economic Statistics*, 2(4):367–374.

Shi, W. and Lee, L.-f. (2016). Identification of spatial durbin panel models. *Journal of Applied Econometrics*, 31(1):133–162.

Shi, W. and Lee, L.-f. (2017). Spatial dynamic panel data models with interactive fixed effects. *Journal of Econometrics*, 197(2):323–347.

Shin, Y. and Thornton, M. (2021). Dynamic network analysis via diffusion multipliers. Working paper, University of York.

Sun, Y. and Malikov, E. (2018). Estimation and inference in functional-coefficient spatial autoregressive panel data models with fixed effects. *Journal of Econometrics*, 203(2):359–378.

Vandenbussche, J., Aghion, P., and Meghir, C. (2006). Growth, distance to frontier and composition of human capital. *Journal of Economic Growth*, 11(2):97–127.

Vogel, J. (2013). Regional Convergence in Europe: A Dynamic Heterogeneous Panel Approach. Mpra paper, University Library of Munich, Germany.

Yang, C. F. (2021). Common factors and spatial dependence: an application to us house prices. *Econometric Reviews*, 40(1):14–50.

Table 1: Estimation results for the SDSF model for EU Regions over 1980-2019

	FE-IV MG		
y^*	0.016	(0.003)	
k	0.460	(0.001)	
k^*	0.252	(0.001)	
	Direct	*Indirect*	*Total*
	0.441	0.286	0.729
CD	357.3	[0.001]	
α	[0.941]	0.972	[1.00]
	CCEX-IV MG		
y^*	0.319	(0.004)	
k	0.440	(0.005)	
k^*	0.315	(0.009)	
	Direct	*Indirect*	*Total*
	0.438	0.758	1.197
CD	12.64	[0.025]	
α	[0.435]	0.501	[0.556]

Notes: We report the estimation results for the SDSF model (28). The spatial fixed effects instrumental variables (FE-IV) estimator takes into account the two-way additive error components, $u_{it} = \alpha_i + \theta_t + \varepsilon_{it}$ whilst the spatial CCEX-IV estimator accommodates the interactive effects, $u_{it} = \alpha_i + \boldsymbol{\lambda}_i' \boldsymbol{\theta}_t + \varepsilon_{it}$. To deal with the endogeneity of the spatial lagged term, y_{it}^*, we employ the de-factored spatial lagged term of the regressor k_t and its square as the IVs for both FE-IV and CCEX-IV estimators. The MG estimators are computed by excluding 17 and 11 regions with $|\hat{\rho}_i| > 1$, for the FE-IV and CCE-IV estimators, respectively. Standard errors are presented in ( ). CD denotes the CSD test proposed by Pesaran (2015), with p-value in [ ] while α is the CSD exponent, proposed by Bailey et al. (2016), with confidence interval at 10% significance in [ ].

Table 2: Descriptive Statistics for CCEX-IV estimates of the SDSF model for EU Regions over 1980–2019

	Median	Mean	SD
ρ	0.350	0.383	0.453
β	0.414	0.439	0.547
π	0.339	0.291	1.110

Notes: Median, mean and standard deviation of individual coefficients are obtained from the CEE-IV estimation results for the SDSF model (28) for the EU Regions over 1980–2019.

Table 3: Descriptive Statistics for HDE, HSI and HSO

	Median	Mean	SD
HDE	0.385	0.418	0.551
HSI	0.850	0.720	1.095
HSO	0.706	0.719	0.489

Notes: Median, mean and standard deviation of heterogeneous direct effects (HDE), heterogeneous spill-in (HSI) and heterogeneous spill-out (HSO) are obtained from the CEE-IV estimation results for the SDSF model (28) for the EU Regions over 1980–2019.

Table 4: Regional efficiency ranking over 1980–2019

$NUTS2_{EU}$	eff	$NUTS2_{EU}$	eff	$NUTS2_{EU}$	eff	$NUTS2_{EU}$	eff
UKI3	1	UKD3	0.3125	UKE1	0.2884	PT17	0.2624
LU00	0.6043	FRJ1	0.3125	BE32	0.2883	EL41	0.2607
BE10	0.5230	DE92	0.3123	EL64	0.2881	AT12	0.2606
NL11	0.4525	ITH4	0.3101	IE04	0.2879	FI19	0.2603
IE06	0.4441	DEA4	0.3101	FRI2	0.2879	ES13	0.2602
UKM7	0.4317	BE24	0.3095	BE25	0.2878	ES41	0.2601
DE60	0.4172	UKK1	0.3090	FRG0	0.2861	DE22	0.2599
UKI4	0.4156	UKF1	0.3089	FRI3	0.2859	ITI3	0.2594
DK01	0.4018	UKL2	0.3071	BE23	0.2851	EL43	0.2590
UKI7	0.3965	AT33	0.3065	FRJ2	0.2851	ES11	0.2589
SE11	0.3918	UKM9	0.3063	NL21	0.2846	FRD2	0.2588
DE71	0.3872	UKE4	0.3052	NL42	0.2842	DE94	0.2583
UKI6	0.3867	ITH5	0.3045	UKE2	0.2838	NL34	0.2582
NL32	0.3867	SE33	0.3037	SE31	0.2827	UKD1	0.2562
IE05	0.3808	AT34	0.3034	DE73	0.2826	ES52	0.2560
UKJ2	0.3710	ES21	0.3016	UKG2	0.2822	ES12	0.2559
ITI4	0.3694	UKJ3	0.3015	FRB0	0.2807	ITI2	0.2558
FR10	0.3681	DE91	0.3014	FRF3	0.2799	UKC1	0.2545
NL31	0.3652	SE23	0.3010	UKM5	0.2792	EL30	0.2522
DE50	0.3603	DEB3	0.3006	BE33	0.2791	FRC2	0.2521
BE21	0.3597	FRL0	0.3001	FRK1	0.2784	UKF3	0.2521
DEA2	0.3517	DE14	0.2996	SE12	0.2784	NL12	0.2515
DK05	0.3510	ITC1	0.2989	ES51	0.2780	UKM8	0.2483
UKD6	0.3509	EL42	0.2987	NL22	0.2780	AT11	0.2472
DEA1	0.3508	DEC0	0.2983	UKH3	0.2779	ES62	0.2462
DE11	0.3493	DEA3	0.2983	ES23	0.2778	ITG1	0.2460
DK04	0.3482	DEA5	0.2980	FRI1	0.2776	BE34	0.2459
ITH1	0.3472	UKK4	0.2971	FRF2	0.2772	UKK3	0.2447
DK03	0.3412	AT31	0.2971	DE24	0.2769	ITF3	0.2446
DE12	0.3399	FRF1	0.2971	FI1D	0.2765	EL63	0.2424
ITH2	0.3377	DE25	0.2968	ITF4	0.2755	ES70	0.2399
DE21	0.3351	DE13	0.2968	AT21	0.2750	ITF2	0.2391
UKJ4	0.3339	ES30	0.2965	DEB1	0.2746	DE93	0.2390
FI1B	0.3339	UKE3	0.2960	DE72	0.2746	PT18	0.2390
UKJ1	0.3331	SE22	0.2957	FRE2	0.2743	ES42	0.2379
AT13	0.3322	UKK2	0.2957	AT22	0.2727	ITF6	0.2361
NL33	0.3313	ITI1	0.2950	ES22	0.2718	UKM6	0.2354
ITC4	0.3293	DK02	0.2943	ES24	0.2686	ES61	0.2335
AT32	0.3286	ITF5	0.2941	DEF0	0.2679	EL53	0.2228
ITH3	0.3261	ITC2	0.2931	DEB2	0.2677	PT11	0.2190
UKH2	0.3252	FI1C	0.2925	DE27	0.2669	PT15	0.2186
UKI5	0.3252	UKL1	0.2913	NL13	0.2665	EL62	0.2169
BE31	0.3251	FRK2	0.2909	FRD1	0.2665	ES43	0.2153
UKG1	0.3247	UKH1	0.2903	SE21	0.2657	ITG2	0.2106
UKD4	0.3205	SE32	0.2901	DE23	0.2655	PT16	0.2037
ITF1	0.3199	FRH0	0.2900	BE35	0.2654	EL51	0.2032
FRM0	0.3196	ITC3	0.2894	ES53	0.2644	EL54	0.1967
UKG3	0.3189	UKC2	0.2893	FRE1	0.2644	UKN0	0.1950
FI20	0.3166	UKD7	0.2889	BE22	0.2637	EL52	0.1900
NL41	0.3165	DE26	0.2889	FRC1	0.2627	EL61	0.1851
UKF2	0.3155					EL65	0.1781

Notes: eff is the time average of individual efficiency estimated by (20). See the Appendix for the NUTS2 regions. See also Notes to Table 1.

Table 5: CCEC-IV MG estimation results for the five efficiency clusters in the EU over 1980–2019

	ρ	β	π	Direct	Indirect	Total
1	0.200	0.547	0.246	0.547	0.079	0.626
	(0.009)	(0.012)	(0.026)			
2	0.352	0.488	0.221	0.488	0.093	0.581
	(0.008)	(0.012)	(0.020)			
3	0.385	0.490	0.334	0.490	0.121	0.611
	(0.006)	(0.014)	(0.016)			
4	0.354	0.444	0.493	0.444	0.143	0.587
	(0.006)	(0.010)	(0.022)			
5	0.349	0.169	0.531	0.170	0.151	0.321
	(0.014)	(0.014)	(0.031)			

Notes: Originally each cluster includes 40 regions but the fifth which contains 42. In order to compute the MG estimates, we exclude the 11 regions with $|\rho_i| > 1$. In particular one region is excluded in the first, the third and the fourth cluster while eight regions are excluded in the fifth cluster. See also Notes to Table 1.

Table 6: Regional efficiency ranking at 1980

$NUTS2_{EU}$	eff	$NUTS2_{EU}$	eff	$NUTS2_{EU}$	eff	$NUTS2_{EU}$	eff
UKI3	1	FRL0	0.36	ES41	0.319	DE27	0.283
NL11	0.873	ITH4	0.36	FRC1	0.319	BE34	0.282
LU00	0.595	ITC1	0.359	NL22	0.318	AT22	0.281
BE10	0.592	DEA5	0.358	DK02	0.318	UKM8	0.281
UKM5	0.568	ES21	0.356	ES11	0.318	UKG2	0.278
SE11	0.526	DEB2	0.356	UKE3	0.317	FI1D	0.278
DE60	0.511	BE32	0.354	ES13	0.316	SE31	0.278
IE06	0.503	FRI2	0.353	BE23	0.316	SE12	0.277
UKI6	0.477	AT13	0.352	SE23	0.316	UKD1	0.277
DK01	0.476	ES23	0.352	SE32	0.315	DE93	0.276
DK05	0.471	UKD3	0.351	BE35	0.314	FI1C	0.275
NL32	0.463	AT32	0.351	BE25	0.313	ES62	0.275
UKI4	0.455	UKJ4	0.349	ITI1	0.312	ES42	0.274
EL42	0.454	ITC4	0.349	AT34	0.311	EL30	0.274
ITH2	0.453	DE14	0.349	SE22	0.31	BE22	0.271
DK04	0.434	NL21	0.347	AT31	0.31	UKC1	0.269
ITH1	0.433	NL41	0.345	ITC2	0.31	UKF3	0.268
EL64	0.431	DEC0	0.344	FRF1	0.309	UKE2	0.267
ITF1	0.43	FRI3	0.343	FRE2	0.308	EL53	0.267
ITI4	0.429	FRH0	0.343	UKM7	0.308	EL51	0.266
BE21	0.429	DE25	0.341	NL34	0.308	DE23	0.265
DEA2	0.421	FRK1	0.341	UKJ3	0.306	AT11	0.265
FR10	0.417	SE33	0.34	UKL2	0.305	AT12	0.265
DEA1	0.417	UKG1	0.338	ES22	0.305	UKD6	0.263
IE05	0.415	UKF1	0.337	ES24	0.304	ES61	0.263
DE50	0.414	FI19	0.334	DE73	0.303	ITI3	0.26
DE11	0.414	FRJ2	0.334	AT21	0.302	UKH3	0.258
DE71	0.413	AT33	0.333	DE26	0.302	FRM0	0.256
UKI5	0.412	FRD1	0.332	UKK1	0.3	PT16	0.254
DE12	0.405	UKC2	0.332	DEF0	0.3	ITI2	0.252
DK03	0.399	EL63	0.331	UKK2	0.299	DE22	0.252
EL41	0.397	UKG3	0.33	ES51	0.298	ITF6	0.25
FRK2	0.396	ES12	0.33	UKE4	0.298	UKD7	0.25
ITH3	0.393	PT17	0.329	ITF4	0.296	EL62	0.247
NL31	0.393	UKF2	0.328	FI1B	0.295	ES70	0.246
NL33	0.392	BE24	0.327	NL42	0.294	FI20	0.245
EL43	0.391	DE91	0.327	ES52	0.294	PT15	0.239
BE31	0.389	ES30	0.326	FRD2	0.294	ITF2	0.238
UKD4	0.387	ITH5	0.325	ITC3	0.293	ITF3	0.238
DE21	0.385	DEB1	0.325	FRC2	0.292	ITG1	0.237
DEB3	0.382	FRI1	0.324	DE72	0.291	EL54	0.236
UKI7	0.382	FRJ1	0.324	UKH1	0.289	UKK3	0.235
FRF2	0.376	UKK4	0.323	UKJ1	0.287	SE21	0.234
IE04	0.376	UKL1	0.322	DE24	0.286	ES43	0.225
DEA3	0.375	UKM9	0.322	UKM6	0.284	EL61	0.222
NL13	0.371	ES53	0.321	FRF3	0.284	EL52	0.215
DE92	0.368	FRB0	0.321	DE94	0.284	ITG2	0.193
UKJ2	0.366	FRG0	0.321	NL12	0.283	EL65	0.179
DEA4	0.365	PT18	0.321	PT11	0.283	UKN0	0.131
ITF5	0.362	BE33	0.32	FRE1	0.283		
DE13	0.36	UKH2	0.319	UKE1	0.283		

Notes: See Notes to Table 4.

Table 7: Regional efficiency ranking at 2019

$NUTS2_{EU}$	eff	$NUTS2_{EU}$	eff	$NUTS2_{EU}$	eff	$NUTS2_{EU}$	eff
UKI3	1.000	BE31	0.267	DE73	0.239		
LU00	0.511	DK04	0.267	ITC3	0.239	IE04	0.209
UKI4	0.414	SE23	0.266	FRG0	0.238	EL30	0.208
BE10	0.411	NL41	0.266	BE23	0.237	ITG1	0.208
IE06	0.406	UKM5	0.265	ES30	0.237	BE35	0.208
IE05	0.390	UKD7	0.263	FRK2	0.237	ITF3	0.207
UKI7	0.355	NL33	0.262	DE13	0.237	FRI2	0.206
FRM0	0.353	UKI5	0.261	UKK4	0.237	ITI2	0.206
UKJ1	0.344	UKE2	0.261	FI1D	0.237	NL12	0.205
UKD6	0.343	DE92	0.260	ITH3	0.236	ES24	0.205
UKJ2	0.335	DE26	0.260	AT21	0.236	FRE2	0.203
DK01	0.332	SE32	0.259	DE27	0.235	FRF3	0.202
NL32	0.329	UKE1	0.259	UKL1	0.235	PT17	0.201
SE11	0.320	DEA5	0.257	DEA3	0.234	FRC2	0.201
FR10	0.317	DEA4	0.256	FRI1	0.234	NL13	0.199
DE50	0.311	SE22	0.256	NL21	0.234	ITF1	0.199
UKH2	0.306	UKF1	0.256	NL22	0.232	ES13	0.198
NL31	0.306	ITI4	0.256	DE72	0.232	ES12	0.198
DE71	0.304	AT33	0.256	ITH2	0.231	ES41	0.196
DE60	0.302	SE12	0.256	FRE1	0.230	ES53	0.196
UKD3	0.292	SE33	0.256	BE33	0.230	DE93	0.195
UKI6	0.292	ES21	0.255	AT12	0.229	ES23	0.194
UKG3	0.291	ITH1	0.255	FRH0	0.229	UKM9	0.192
DE91	0.291	NL42	0.255	ITH4	0.229	DEB2	0.192
NL11	0.289	UKK2	0.254	BE22	0.229	ES52	0.187
DEA1	0.289	DEC0	0.254	FRD2	0.227	ITF2	0.186
DE11	0.286	DE25	0.254	ES51	0.225	ITF6	0.186
FI1B	0.285	UKG2	0.254	ES22	0.225	ITG2	0.185
UKK1	0.284	UKN0	0.253	DEB1	0.225	BE34	0.183
UKG1	0.283	FI1C	0.252	UKK3	0.224	ES43	0.180
AT32	0.283	UKC2	0.252	UKC1	0.224	ES62	0.179
BE21	0.283	DE24	0.251	ITC2	0.224	ES70	0.179
DE21	0.282	UKD1	0.250	FRJ1	0.223	EL42	0.179
AT34	0.281	UKH1	0.250	FRI3	0.223	ES61	0.175
UKJ4	0.280	AT22	0.250	BE32	0.223	ES42	0.171
DEA2	0.280	DE14	0.249	FRF1	0.222	PT15	0.166
UKE4	0.279	FI20	0.249	DE94	0.222	EL62	0.166
UKM7	0.277	UKE3	0.249	ITC1	0.220	PT18	0.159
UKJ3	0.277	UKM8	0.248	DEF0	0.219	EL65	0.159
AT13	0.277	DE22	0.247	FRB0	0.218	PT16	0.156
UKD4	0.276	ITH5	0.247	ITI3	0.218	PT11	0.156
DK03	0.275	DK05	0.247	FRF2	0.218	EL53	0.155
UKF2	0.273	DK02	0.245	FRK1	0.218	EL43	0.153
BE24	0.271	FRJ2	0.244	FRC1	0.216	EL63	0.147
UKL2	0.270	DE23	0.243	ITF5	0.216	EL52	0.143
ITC4	0.269	ITI1	0.242	ITF4	0.215	EL41	0.141
SE21	0.269	DEB3	0.241	AT11	0.215	EL54	0.141
UKH3	0.268	FI19	0.241	ES11	0.213	EL64	0.140
DE12	0.268	UKM6	0.240	NL34	0.212	EL51	0.138
SE31	0.268	FRL0	0.240	UKF3	0.212	EL61	0.137
AT31	0.267	BE25	0.240	FRD1	0.209		

Notes: See Notes to Table 4.

Table 8: Quintile Direct, Spill-in, Spill-out effects of production input

	Quintile Connectedness Matrix				
	1	2	3	4	5
1	0.591	0.100	0.114	0.100	0.058
2	0.130	0.648	0.173	0.170	0.098
3	0.151	0.194	0.692	0.198	0.122
4	0.176	0.216	0.226	0.664	0.144
5	0.137	0.160	0.176	0.178	0.351
QSI	0.372	0.570	0.665	0.762	0.650
QSO	0.594	0.670	0.688	0.646	0.421
QNE	0.222	0.100	0.023	-0.116	-0.229

Notes: QSI is the spill-in effect, QSO is the spill-out effect and QNE is the net effect defined as difference between QSO and QSI across the five efficiency clusters.

Figure 1: Kernel density of ρ, β and π

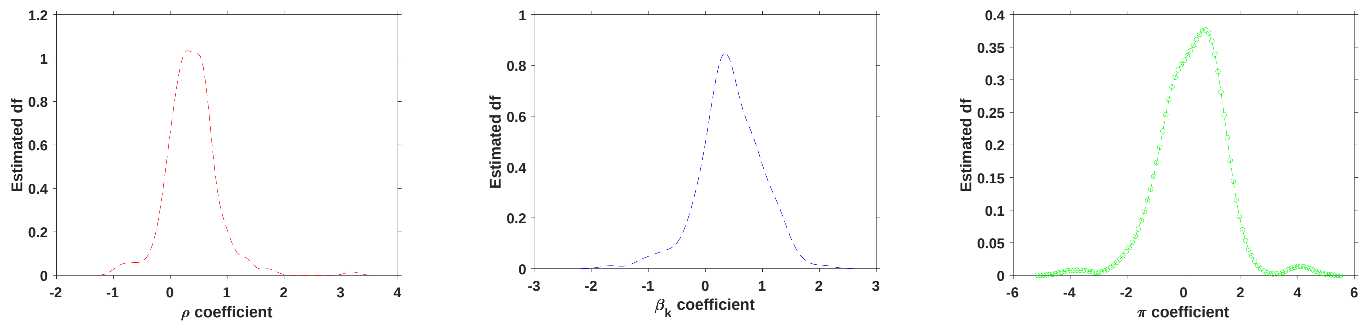

Figure 2: The spatial distribution of $\hat{\rho}_i$ among EU regions

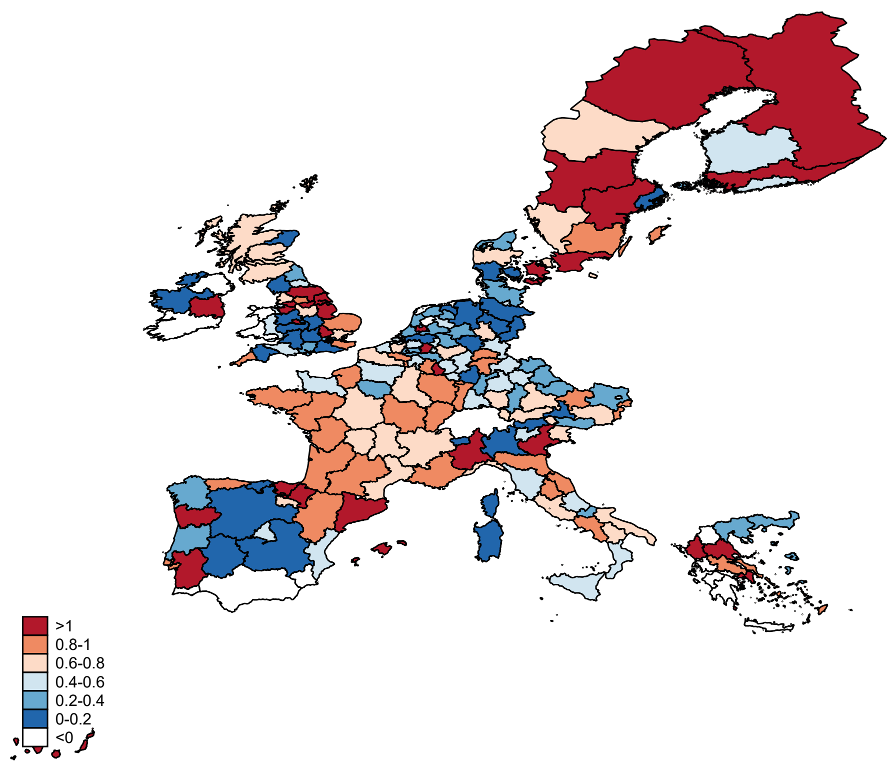

Figure 3: The spatial distribution of $\hat{\beta}_i$ among EU regions

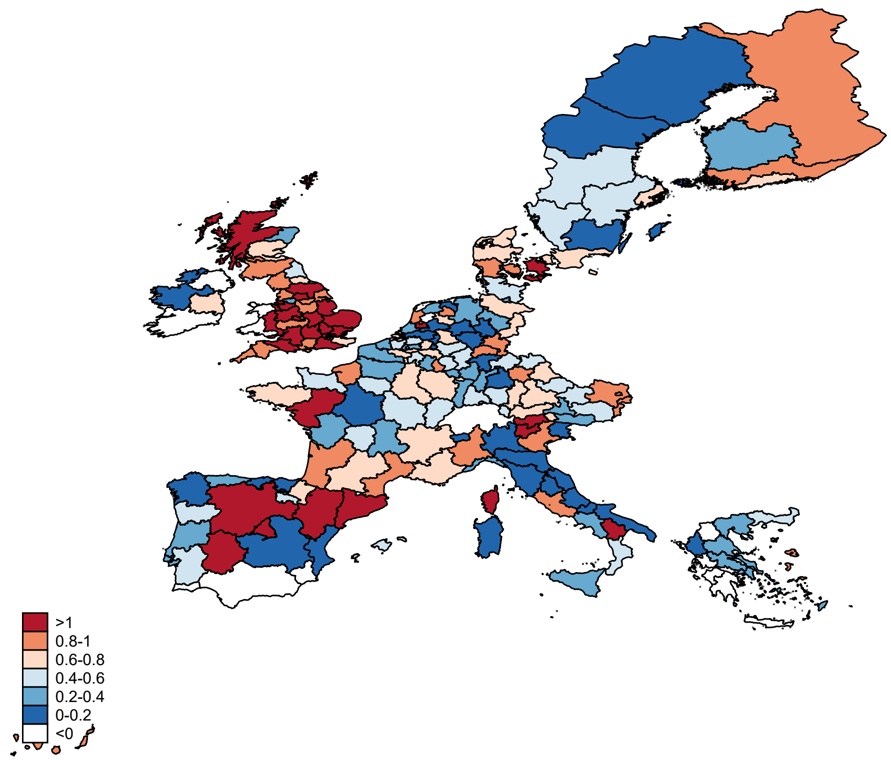

Figure 4: The spatial distribution of $\hat{\pi}_i$ among EU regions

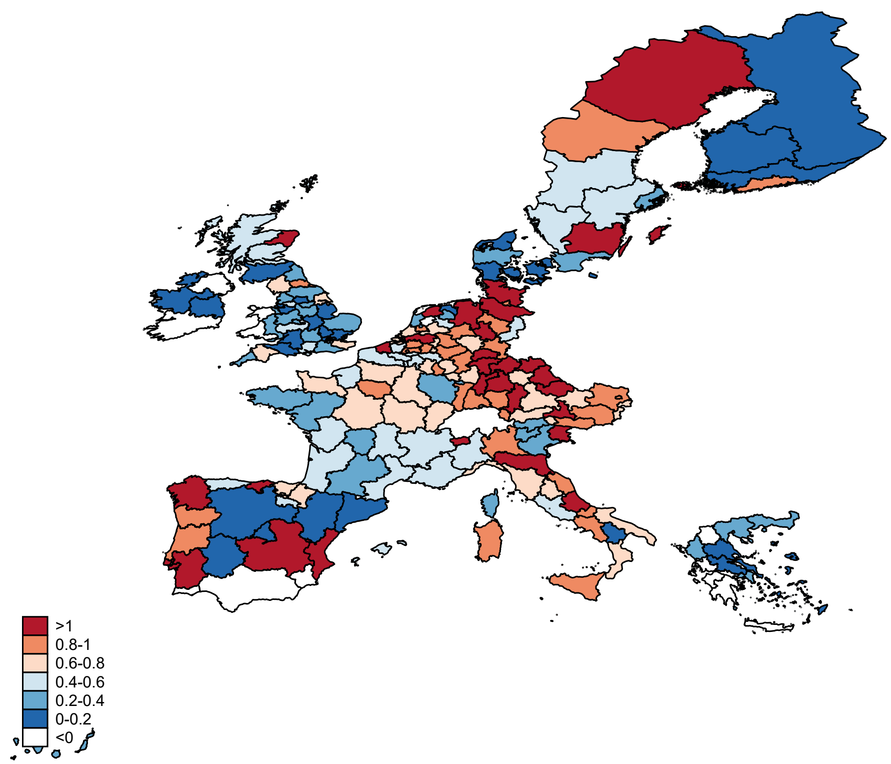

Figure 5: Kernel density of HDE, HSI and HSO

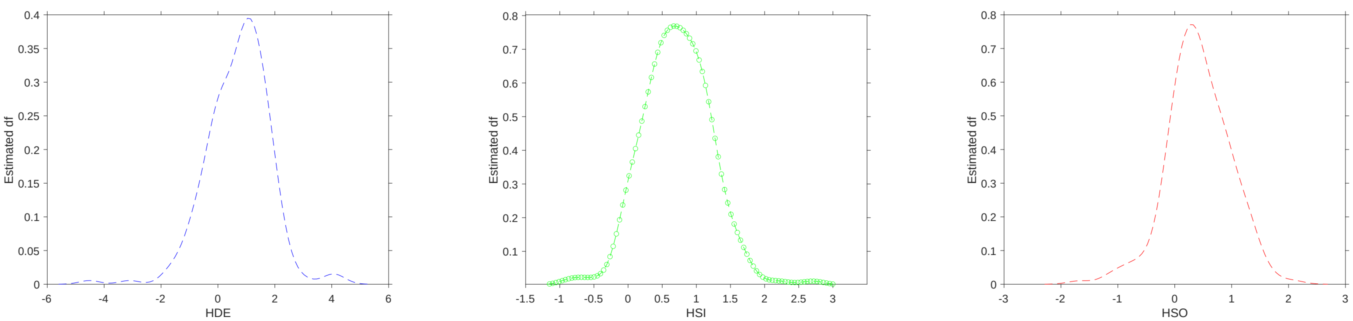

Figure 6: The spatial distribution of HDE of capital intensity on labour productivity among EU regions

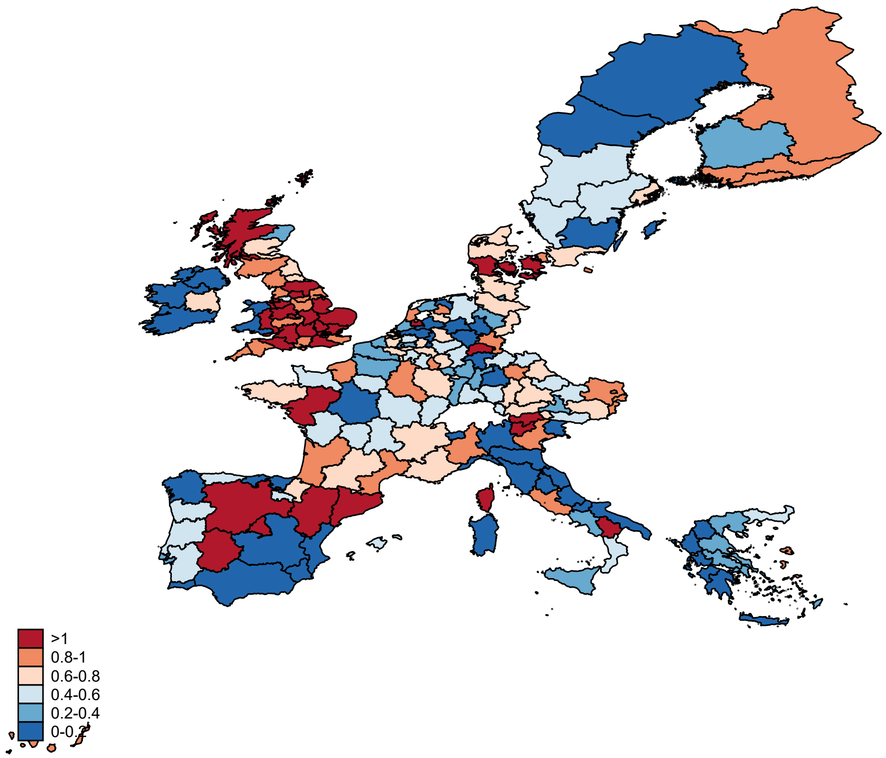

Figure 7: The spatial distribution of HSI and HSO of capital intensity on labour productivity among EU regions

(a) HSI

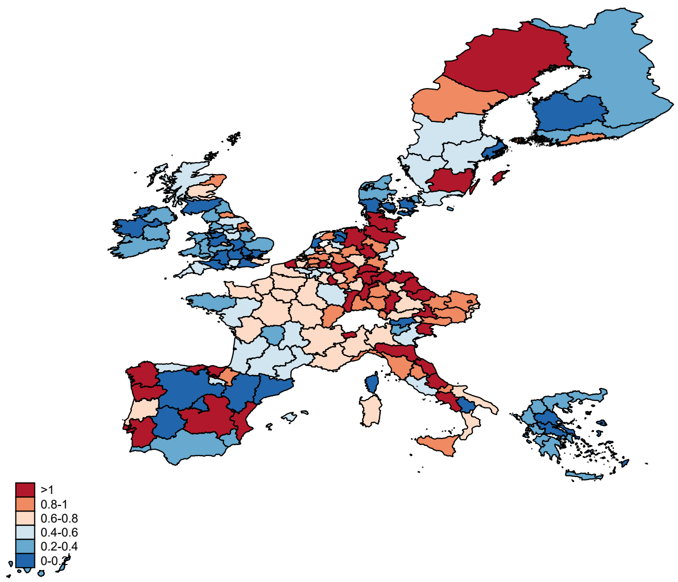

(b) HSO

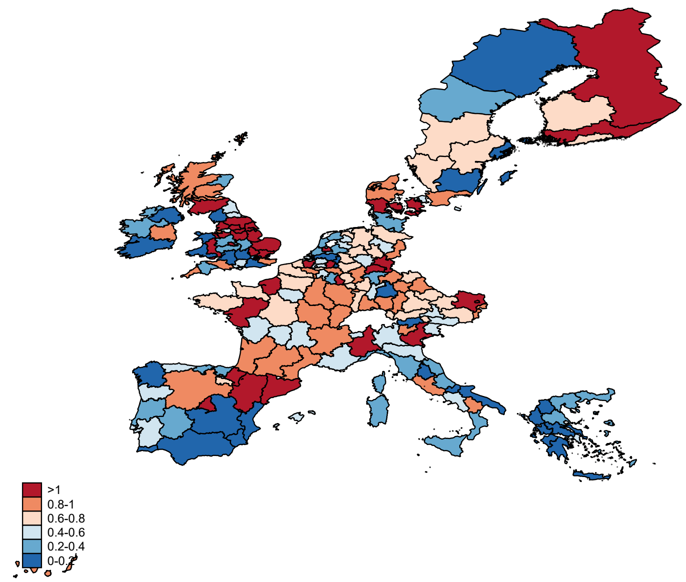

Figure 8: The distribution of the five efficiency clusters across countries

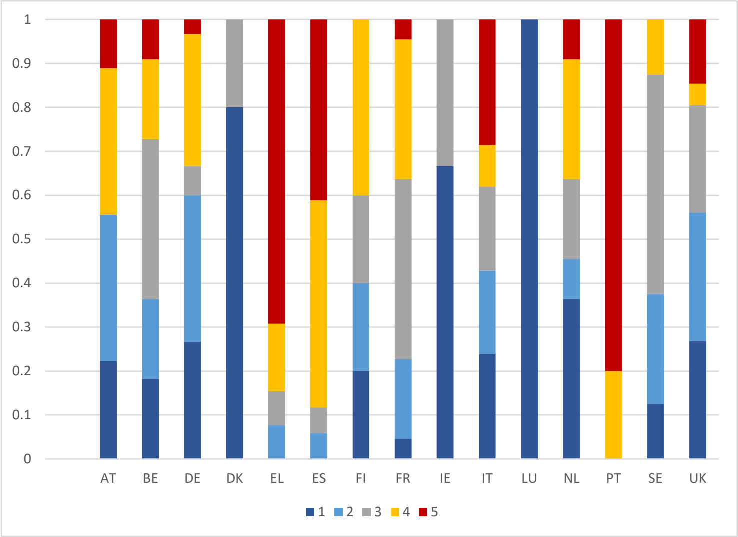

Notes: 1-5 denote the five efficiency clusters from the best (1) to the worst (5).

Figure 9: The spatial distribution of technical efficiency among EU regions

(a) 1980 (b) 2019

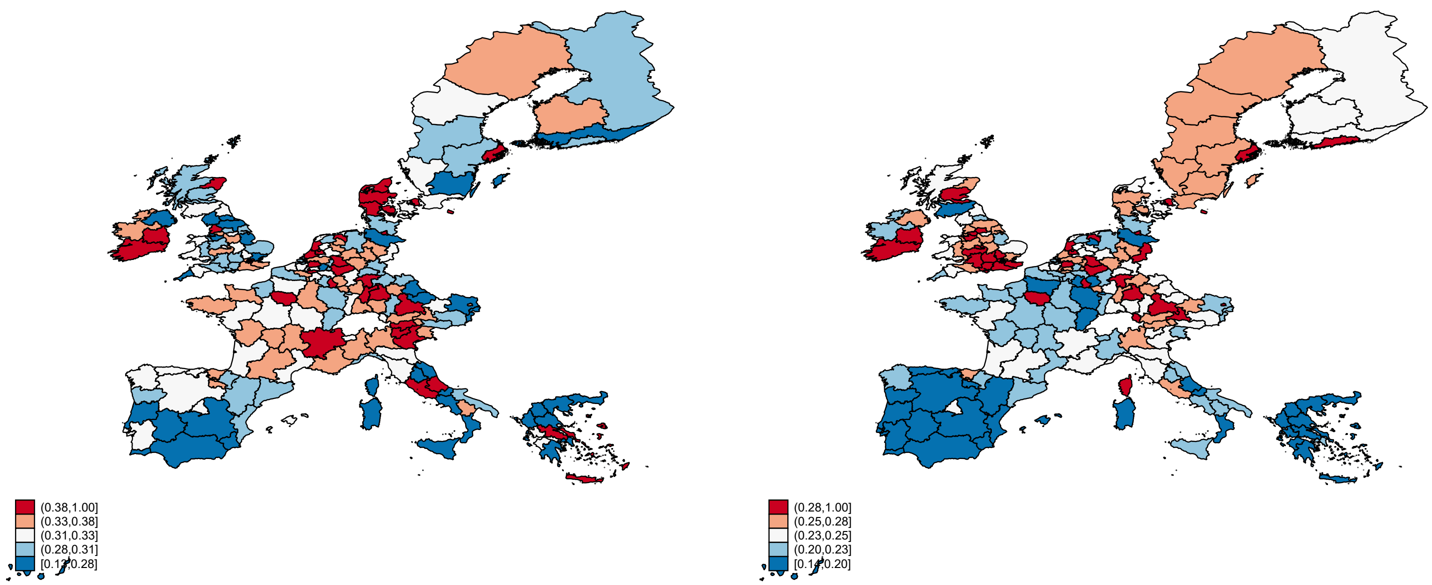

Figure 10: The spatial distribution of per capita GDP among EU regions

(a) 1980

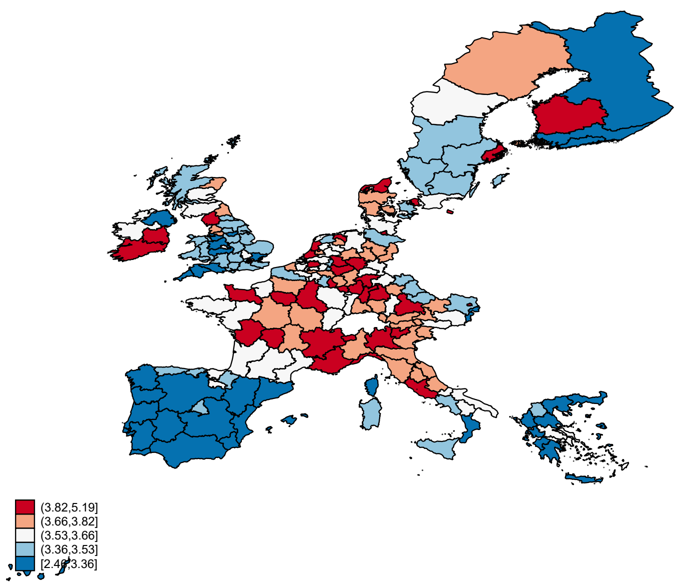

(b) 2019

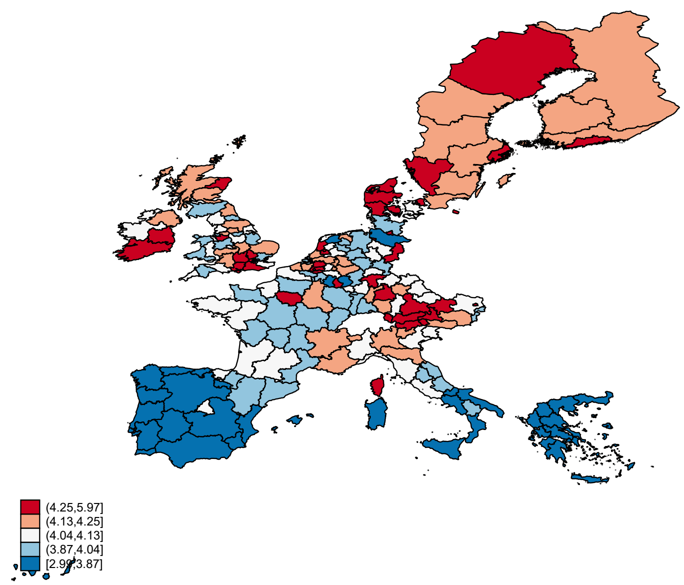

Figure 11: GDP per capita Quintile Ratios (QR) across the five efficiency clusters

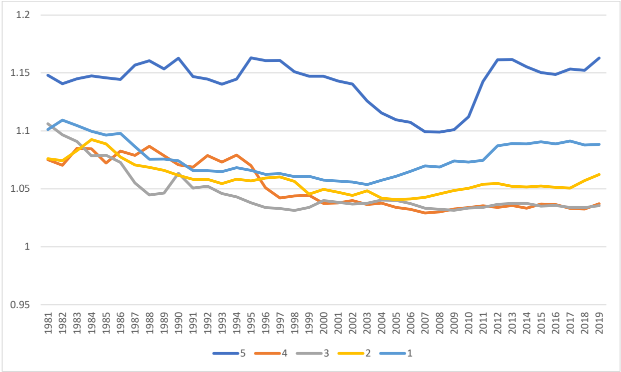

The QR are calculated for each efficiency cluster, from the most efficient (1) to the least efficient (5) and show the ratio of the GDP of the regions with the highest GDP (the top quintile, the 20%) to that of the regions with the lowest GDP (the bottom quintile, the 20%).

Figure 12: The transition probability matrix (TM) across the five efficiency clusters

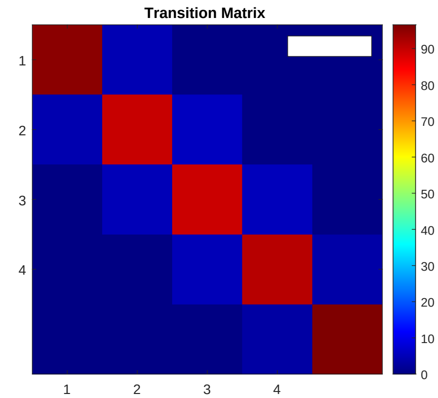

The transition probability matrix shows the probability of the regions of moving across five efficiency cluster over time. The TM becomes an identity matrix in case of perfect immobility (probability equal to one) and a matrix with zeros on the diagonal in case of perfect mobility (probability equal to zero).

Figure 13: The GCM analysis of the five efficiency clusters

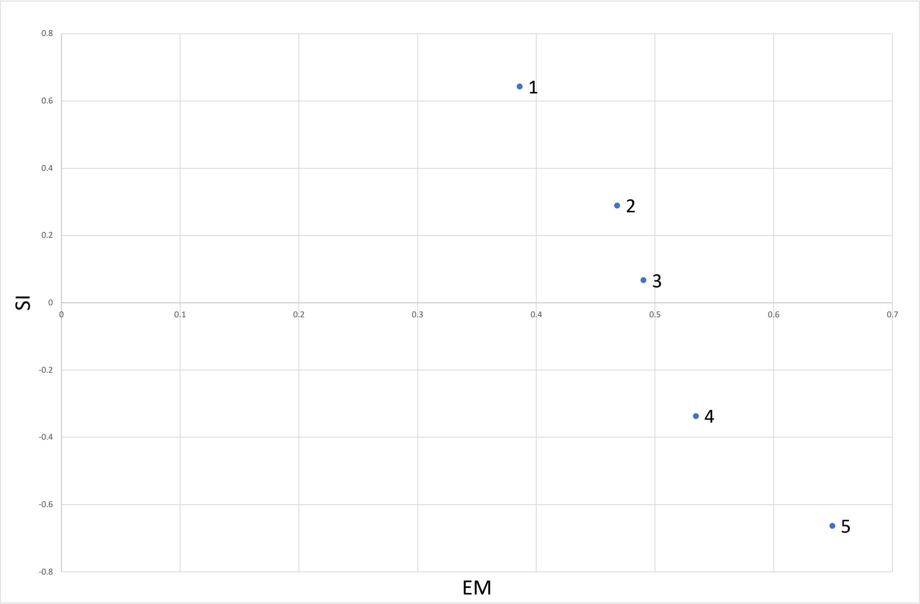

Notes: EM is External Motivation, SI denotes Systemic Influence for five clusters from the most efficient 1 to the least efficient 5.

6 Appendix

Table 9: Names and codes of the 202 NUTS2 regions

Codes	Names	Codes	Names
AT11	Burgenland	DK01	Hovedstaden
AT12	Niederösterreich	DK02	Sjælland
AT13	Wien	DK03	Syddanmark
AT21	Kärnten	DK04	Midtjylland
AT22	Steiermark	DK05	Nordjylland
AT31	Oberösterreich	EL30	Attiki
AT32	Salzburg	EL41	Voreio Aigaio
AT33	Tirol	EL42	Notio Aigaio
AT34	Vorarlberg	EL43	Kriti
BE10	Région de Bruxelles-Capitale	EL51	Anatoliki Makedonia, Thraki
BE21	Prov. Antwerpen	EL52	Kentriki Makedonia
BE22	Prov. Limburg	EL53	Dytiki Makedonia
BE23	Prov. Oost-Vlaanderen	EL54	Ipeiros
BE24	Prov. Vlaams-Brabant	EL61	Thessalia
BE25	Prov. West-Vlaanderen	EL62	Ionia Nisia
BE31	Prov. Brabant wallon	EL63	Dytiki Ellada
BE32	Prov. Hainaut	EL64	Sterea Ellada
BE33	Prov. Liège	EL65	Peloponnisos
BE34	Prov. Luxembourg	ES11	Galicia
BE35	Prov. Namur	ES12	Principado de Asturias
DE11	Stuttgart	ES13	Cantabria
DE12	Karlsruhe	ES21	País Vasco
DE13	Freiburg	ES22	Comunidad Foral de Navarra
DE14	Tübingen	ES23	La Rioja
DE21	Oberbayern	ES24	Aragón
DE22	Niederbayern	ES30	Comunidad de Madrid
DE23	Oberpfalz	ES41	Castilla y León
DE24	Oberfranken	ES42	Castilla-la Mancha
DE25	Mittelfranken	ES43	Extremadura
DE26	Unterfranken	ES51	Cataluña
DE27	Schwaben	ES52	Comunidad Valenciana
DE50	Bremen	ES53	Illes Balears
DE60	Hamburg	ES61	Andalucía
DE71	Darmstadt	ES62	Región de Murcia
DE72	Gießen	ES70	Canarias
DE73	Kassel	FI19	Länsi-Suomi
DE91	Braunschweig	FI1B	Helsinki-Uusimaa
DE92	Hannover	FI1C	Etelä-Suomi
DE93	Lüneburg	FI1D	Pohjois- ja Itä-Suomi
DE94	Weser-Ems	FI20	Åland
DEA1	Düsseldorf	FR10	Île de France
DEA2	Köln	FRB0	Centre - Val de Loire
DEA3	Münster	FRC1	Bourgogne
DEA4	Detmold	FRC2	Franche-Comté
DEA5	Arnsberg	FRD1	Basse-Normandie
DEB1	Koblenz	FRD2	Haute-Normandie
DEB2	Trier	FRE1	Nord-Pas-de-Calais
DEB3	Rheinhessen-Pfalz	FRE2	Picardie
DEC0	Saarland	FRF1	Alsace
DEF0	Schleswig-Holstein	FRF2	Champagne-Ardenne

Table 10: Names and codes of the 202 NUTS2 regions -continued

FRF3	Lorraine	PT17	Área Metropolitana de Lisboa
FRG0	Pays-de-la-Loire	PT18	Alentejo
FRH0	Bretagne	SE11	Stockholm
FRI1	Aquitaine	SE12	Östra Mellansverige
FRI2	Limousin	SE21	Småland med öarna
FRI3	Poitou-Charentes	SE22	Sydsverige
FRJ1	Languedoc-Roussillon	SE23	Västsverige
FRJ2	Midi-Pyrénées	SE31	Norra Mellansverige
FRK1	Auvergne	SE32	Mellersta Norrland
FRK2	Rhône-Alpes	SE33	Övre Norrland
FRL0	Provence-Alpes-Côte d'Azur	UKC1	Tees Valley and Durham
FRM0	Corse	UKC2	Northumberland and Tyne and Wear
IE04	Northern and Western	UKD1	Cumbria
IE05	Southern	UKD3	Greater Manchester
IE06	Eastern and Midland	UKD4	Lancashire
ITC1	Piemonte	UKD6	Cheshire
ITC2	Valle d'Aosta/Vallée d'Aoste	UKD7	Merseyside
ITC3	Liguria	UKE1	East Yorkshire and Northern Lincolnshire
ITC4	Lombardia	UKE2	North Yorkshire
ITF1	Abruzzo	UKE3	South Yorkshire
ITF2	Molise	UKE4	West Yorkshire
ITF3	Campania	UKF1	Derbyshire and Nottinghamshire
ITF4	Puglia	UKF2	Leicestershire, Rutland and Northamptonshire
ITF5	Basilicata	UKF3	Lincolnshire
ITF6	Calabria	UKG1	Herefordshire, Worcestershire and Warwickshire
ITG1	Sicilia	UKG2	Shropshire and Staffordshire
ITG2	Sardegna	UKG3	West Midlands
ITH1	Provincia Autonoma di Bolzano/Bozen	UKH1	East Anglia
ITH2	Provincia Autonoma di Trento	UKH2	Bedfordshire and Hertfordshire
ITH3	Veneto	UKH3	Essex
ITH4	Friuli-Venezia Giulia	UKI3	Inner London - West
ITH5	Emilia-Romagna	UKI4	Inner London - East
ITI1	Toscana	UKI5	Outer London - East and North East
ITI2	Umbria	UKI6	Outer London - South
ITI3	Marche	UKI7	Outer London - West and North West
ITI4	Lazio	UKJ1	Berkshire, Buckinghamshire and Oxfordshire
LU00	Luxembourg	UKJ2	Surrey, East and West Sussex
NL11	Groningen	UKJ3	Hampshire and Isle of Wight
NL12	Friesland	UKJ4	Kent
NL13	Drenthe	UKK1	Gloucestershire, Wiltshire and Bristol/Bath area
NL21	Overijssel	UKK2	Dorset and Somerset
NL22	Gelderland	UKK3	Cornwall and Isles of Scilly
NL31	Utrecht	UKK4	Devon
NL32	Noord-Holland	UKL1	West Wales and The Valleys
NL33	Zuid-Holland	UKL2	East Wales
NL34	Zeeland	UKM5	North Eastern Scotland
NL41	Noord-Brabant	UKM6	Highlands and Islands
NL42	Limburg	UKM7	Eastern Scotland
PT11	Norte	UKM8	West Central Scotland
PT15	Algarve	UKM9	Southern Scotland
PT16	Centro	UKN0	Northern Ireland